HIGH-LATITUDE OCEAN AND SEA ICE SURFACE FLUXES: CHALLENGES FOR CLIMATE RESEARCH

by Mark A. Bourassa, Sarah T. Gille, Cecilia Bitz, David Carlson, Ivana Cerovecki, Carol Anne Clayson, Meghan F. Cronin, Will M. Drennan, Chris W. Fairall, Ross N. Hoffman, Gudrun Magnusdottir, Rachel T. Pinker, Ian A. Renfrew, Mark Serreze, Kevin Speer, Lynne D. Talley, and Gary A. Wick

High latitudes present extreme conditions for the measurement and estimation of air–sea and ice fluxes, limiting understanding of related physical processes and feedbacks that are important elements of the Earth's climate.

High-latitude climate change can manifest itself in astonishing ways. Arctic sea ice extent at the end of the melt season in September is declining at a mean rate of 12% per decade, with record seasonal minima in 2007 and 2012 (Comiso et al. 2008; Shawstack 2012). In 2001/02, the Larsen B Ice Shelf on the Antarctic Peninsula collapsed in a matter of months (Rignot et al. 2004), and in 2008, the Wilkins Ice Shelf collapsed equally quickly (Scambos et al. 2009). Ocean heat content is rising rapidly in high-latitude regions of both hemispheres (e.g., Gille 2002; Karcher et al. 2003; Bindoff et al. 2007; Purkey and Johnson 2010). The observed trends are expected to continue and are broadly consistent with projections of anthropogenic climate change reported in the Intergovernmental Panel on Climate Change (IPCC) Fourth Assessment Report (AR4) (Randall et al. 2007). A common element in high-latitude climate changes is a dependence on surface fluxes;
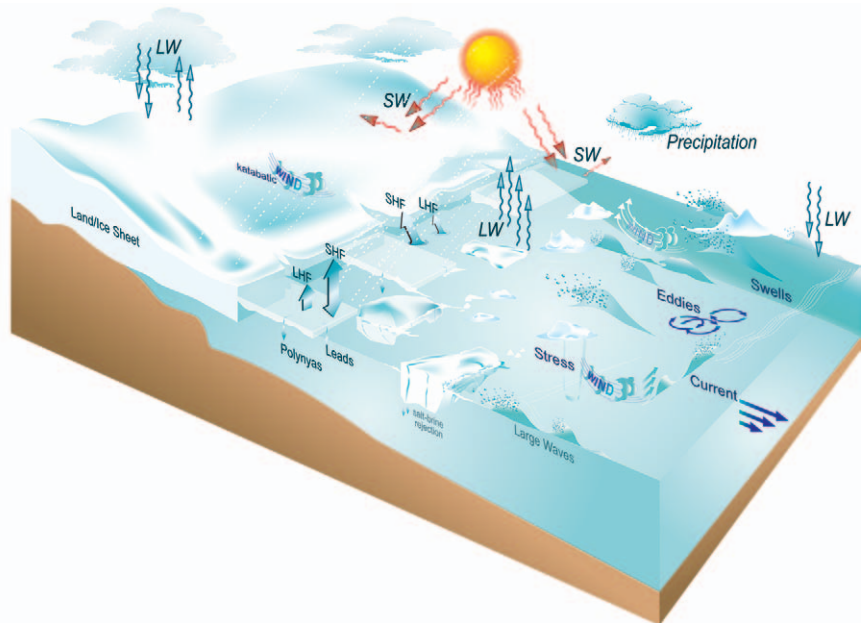

Fig. 1. Schematic of surface fluxes and related processes for high latitudes. Radiative fluxes are both SW and LW. Surface turbulent fluxes are stress, SHF, and LHF. Ocean surface moisture fluxes are *P* and *E* (proportional to LHF). Processes specific to high-latitude regimes can strongly modulate fluxes. These include strong katabatic winds, effects due to ice cover and small-scale open patches of water associated with leads and polynyas, air–sea temperature differences that vary on the scale of eddies and fronts (i.e., on the scale of the oceanic Rossby radius, which can be short at high latitudes), deep and bottom water formation, and enhanced freshwater input associated with blowing snow.

we focus on the exchange of energy, momentum, and material between the ocean and atmosphere and between atmosphere and sea ice (the basic concepts defining surface fluxes are outlined in "Primer: What is an air–sea flux?"). Surface fluxes at high latitudes

PRIMER: WHAT IS AN AIR–SEA FLUX?

Air–sea fluxes represent the exchange of energy and material between the ocean and lower atmosphere. They include the net fluxes of momentum (stress) from wind, energy (downward and reflected shortwave radiation, downward and emitted longwave radiation, latent heat flux, and sensible heat flux), and mass (Fig. 1). Mass fluxes encompass a broad number of variables, including moisture (precipitation and deposition, evaporation or sublimation, and runoff or ice melt) and gases (e.g., CO_2), as well as atmospheric aerosols (solid or liquid particles), which can, for example, supply salt to the atmosphere, provide chlorine that can contribute to ozone depletion, or deliver iron-rich dust derived on land to the ocean, spurring biological growth.

Wind stress, sensible and latent heat fluxes, gas and aerosol exchange, and evaporation are classified as turbulent fluxes. These fluxes depend on nonlinear, covarying terms, meaning that random errors in bulk variables can have a rectified effect, causing significant errors even in large-scale averaged fields. Depending on the space and time scales being investigated (Fig. 3), these fluxes could be averaged over a wide range of surface and meteorological conditions. Turbulent fluxes on the time scales of intense storms (roughly one day) can be very large compared to long-term averages. Although turbulent fluxes can be measured directly, they are typically parameterized (see Table 1) (e.g., Curry et al. 2004). At high latitudes, low-level winds are associated with intense storms from small (polar lows) to large (warm-core seclusions) scales, and they can be enhanced by orography (e.g., low-level jets around Greenland) and reduced friction over some types of ice, leading to intense katabatic winds (e.g., from the Antarctic continent), and consequently strong air–sea momentum exchange along coastlines. Openings in the ice (i.e., leads and polynyas) can lead to small-spatial-scale variations in air–sea turbulent heat fluxes, with greatly enhanced exchange of heat over open water (Fig. 1). Small-scale ocean currents and eddies can also modify turbulent heat fluxes.

Radiative fluxes at the surface include downwelling and upwelling (reflected) shortwave radiation originating from the sun as well as downwelling and upwelling longwave radiation emitted by the atmosphere and the surface, respectively (e.g., Petty 2006) Radiative fluxes exhibit unique characteristics at high latitudes.

are important to processes in the ocean (e.g., deep convection, dynamics of the Southern Ocean and the Greenland–Iceland–Norwegian Seas, water mass transformation), the cryosphere (warming of waters, ice transport, and cloud formation), and the atmosphere (cloud modification of radiative fluxes, feedbacks to annular modes), and have variability associated with a broad range of processes, as depicted schematically in Fig. 1. However, the magnitude and variations of surface fluxes at high latitudes are poorly known, contributing to the present large uncertainty in estimates of the high-latitude climate of the ocean and lower atmosphere (e.g., Dong et al. 2007; Vancoppenolle et al. 2011; Kwok and Untersteiner 2011; Cerovecki et al. 2011, 2013), and limiting our ability to validate climate models used to project twenty-first-century climate (e.g., Christensen et al. 2007). Improving our knowledge of high-latitude surface fluxes will require close collaboration among meteorologists, oceanographers, ice physicists, and climatologists, and between observationalists and modelers, as well as new combinations of in situ measurements and satellite remote sensing [e.g., improvements on ideas discussed by Bourassa et al. (2010b)].

This article, an outcome of the U.S. Climate Variability and Predictability (CLIVAR) Working Group on High Latitude Surface Fluxes Workshop (www.usclivar.org/hlat.php), describes the scientific requirements for surface fluxes at high latitudes, which

AFFILIATIONS: Bourassa, Clayson,* and Speer—The Florida State University, Tallahassee, Florida; Gille, Cerovecki, and Talley—University of California, San Diego, La Jolla, California; Bitz—University of Washington, Seattle, Washington; Carlson—British Antarctic Survey, Cambridge, United Kingdom; Cronin—NOAA/Pacific Marine Environmental Laboratory, Seattle, Washington; Drennan—University of Miami, Miami, Florida; Fairall and Wick—NOAA/Earth System Research Laboratory, Boulder, Colorado; Hoffman—Atmospheric and Environmental Research, Lexington, Massachusetts; Magnusdottir—University of California, Irvine, Irvine, California; Pinker—University of Maryland, College Park, College Park, Maryland; Renfrew—University of East Anglia, Norwich, United Kingdom; Serreze—University of Colorado, Boulder, Colorado

*CURRENT AFFILIATION: Woods Hole Oceanographic Institution, Woods Hole, Massachusetts

CORRESPONDING AUTHOR: Sarah Gille, Scripps Institution of Oceanography, University of California, San Diego, 9500 Gilman Dr., Mail Code 0230, La Jolla, CA 92093-0230
E-mail: sgille@ucsd.edu

They are not expressed using simple bulk formulas and are therefore not included in Table 1. All the radiative fluxes vary with cloud cover and aerosol amount and characteristics. For the downwelling shortwave, the major modulators at high latitudes are the solar angle and the surface albedo (i.e., the fraction of incident radiation that is reflected). Surface albedo varies strongly between ice, snow, and water, and this is further complicated by temporal surface variability during melt periods and by darkening due to dust and carbonaceous aerosol deposition. Downwelling longwave radiation is controlled largely by cloud cover, which is high at high latitudes, cloud-base height, which is often low at high latitudes, and by water vapor concentration, which is small at high latitudes. The upwelling longwave radiation depends on surface skin temperature, which differs widely between the ice and the open-water bodies and is not well known in areas with ice. Furthermore, small changes in shortwave reflectivity and longwave emissivity can alter the energy budget sufficiently to cause substantial growth or melting of ice.

Net freshwater fluxes into a volume of the ocean are determined by oceanic transport, runoff (including melting land ice), precipitation (P, which includes rain and snow), and evaporation (E). The latter two are often viewed in the combined term of net precipitation, or $P - E$. An important factor for ocean freshwater and salinity balances in regions with sea ice is the fractionation of water and salt in a process called brine rejection: sea ice is greatly depleted in salt, and most of the salt enters the underlying seawater, where it increases the seawater density. When the sea ice melts, the resulting seawater is significantly freshened and hence lighter. When sea ice, which can be thought of as seawater of very low salinity, is transported from one region to another, an advective freshwater flux between the regions arises. Ice and brine formation are modulated locally by the intermixed areas of open water, organic slicks, new ice, existing bare ice, snow-covered ice, and melt ponds; these interact radiatively with overlying regions of haze, low cloud, and clear sky. Furthermore, deposition of particles (e.g., of black carbon) and gases (e.g., of mercury) affect the surface radiative properties (e.g., albedo). Thus, subtle changes in heat or momentum fluxes cause, and respond to, rapid water phase change.

we define as including the Arctic/subarctic Ocean and the Southern Ocean. We inventory the reasons, both logistical and physical, why existing flux products do not meet these requirements. We conclude with suggestions for improving high-latitude flux estimates. Our focus is on ocean–atmosphere fluxes and radiative fluxes over high-latitude seas and sea ice. We do not endeavor to replicate material in the recent Snow, Water, Ice, Permafrost in the Arctic (SWIPA) assessment (AMAP 2011, www.amap.no/swipa/), which provides an up-to-date description of surface and lateral fluxes and net mass changes of the Greenland ice sheet, and addresses requirements for measuring carbon fluxes over tundra and terrestrial permafrost regions.

UNIQUE CHALLENGES AND DESIRED ACCURACIES.

High-latitude fluxes differ markedly from those in temperate regions. As depicted in Fig. 1, fluxes are influenced by the presence of ice, frequent high wind speeds (Fig. 2), low winter temperatures, both large and small seasonal

FIG. 2. Frequency of winds exceeding 25 m s^{-1} for the QuikSCAT observations from Jul 1999 through Jun 2009, based on Remote Sensing Systems' Ku2001 algorithm. Statistics are computed by averaging vector winds from the original satellite swath measurements into 0.25° × 0.25° bins. Poleward of roughly 55° neighboring orbits overlap and only one of the two observations is considered. Northern Hemisphere extreme winds are associated with topography (e.g., around Greenland; see Renfrew et al. 2008) and western boundary currents, and occur in boreal winter; Southern Hemisphere events are more widespread and occur year-around. Locations with less than approximately 51% of possible observations are plotted as white, thereby excluding some regions with too much seasonal ice.

temperature ranges, and pronounced variability on local scales, particularly along sea ice margins and leads (linear openings in the ice cover) or in
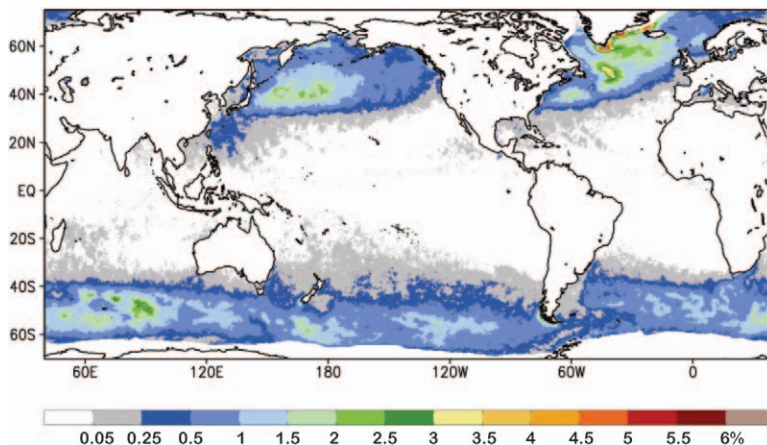
association with mesoscale eddies. As a result, physical understanding gained in temperate regions is not necessarily applicable to high latitudes.

The high-latitude environment also poses logistical challenges. Capturing an annual cycle in fluxes, for example, requires that instruments function through long periods of cold polar darkness, often far from support services, in situations subject to icing and extreme wave conditions. These logistical challenges are reflected in a relative paucity of standard surface and upper-air meteorological data and an almost complete absence of moored[1] or free-drifting sensor systems in large areas of the polar oceans, particularly those covered with seasonal or perennial ice. Frequent cloud cover in high latitudes restricts the availability of surface and atmospheric information derived from visible and infrared (IR) wavelength satellite observations. Moreover, most current visible and IR sensors have difficulty distinguishing clouds from snow or ice cover. This lack of information as well as uncertainties in the parameterizations of fluxes reduces the quality of data assimilation

---

[1] The first meteorological mooring in the Southern Ocean was deployed in March 2010, at 47°S, 140°E, by the Australian Integrated Marine Observing System (Trull et al. 2010). It measures wind, temperature, humidity, atmospheric pressure, solar radiation, and precipitation but not turbulent fluxes. A second mooring that was deployed in the Agulhas Return Current at 38.5°S, 30°E in November 2010 broke loose from its anchor after less than seven weeks. Similar difficulties occurred in the northern high latitudes (Moore et al. 2008).

EXAMPLES: SURFACE FLUXES FROM A CLIMATE RESEARCH PERSPECTIVE

Surface flux products are widely used in the fields of oceanography, glaciology, sea ice dynamics, and atmospheric dynamics. Science questions address time scales from less than an hour to decades or longer, resulting in a diversity of accuracy requirements. Here we provide a few examples.

From a long-term climate change perspective. Over the last few decades, a number of aspects of the climate system have changed substantially. In the ocean, observed long-term warming trends from 1993 to 2003 can be explained by a mean energy flux into the ocean of just 0.86 ± 0.12 W m^{-2} (Hansen et al. 2005). For sea ice, a 1 W m^{-2} flux imbalance equates to a 10-cm ice melt in a year, a significant fraction of the ice budget. Basin-scale changes in ocean salinity associated with global change correspond to small changes in air–sea freshwater flux on the order of 0.05 practical salinity unit (psu) decade^{-1} (Boyer et al. 2005) concentrated in the top 200 m. This is equivalent to a change in liquid $P - E$ of 3 cm yr^{-1}. Similarly, North Atlantic freshwater flux anomalies sufficient to slow deep convection (Curry and Mauritzen 2005) derive from river runoff and ice melt, and are equivalent to $P - E$ of almost 1 cm yr^{-1} over the area of the Arctic and North Atlantic. These climate change signals of $O(1$ W m$^{-2})$ for heat and $O(1$ cm yr$^{-1})$ for freshwater are far below any currently estimated observational accuracy globally or in polar regions, even in averaged estimates computed from many independent samples. Hence, long-term changes in these fluxes are more effectively diagnosed by observing the ocean temperature and salinity changes as integrators of heat and freshwater fluxes (e.g., Hansen et al. 2005; Levitus et al. 2005; Boyer et al. 2005, 2007; Domingues et al. 2008; Wunsch et al. 2007; Hosoda et al. 2009; Levitus et al. 2009; Durack and Wijffels 2010). Capabilities of current observing systems should not be a deterrent to efforts at improvement; significant scientific gains could be made if the uncertainty in heat and freshwater flux estimates (as crudely estimated by the spread in modern products, cf. Fig. 5) could be improved by an order of magnitude and if available products were consistently released with high-quality uncertainty and bias information.

From an open-ocean circulation perspective. When sea ice is not involved, the open-ocean circulation is driven primarily by wind stress curl patterns that deform sea level and thermocline fields, and by heat and moisture fluxes that alter water density. Since the curl patterns are caused in large part by zonal and meridional variations in the wind direction (e.g., easterly trades in the tropics, westerly jet stream at midlatitudes), from the ocean circulation perspective it is necessary to resolve not only the wind stress magnitude but also its direction. Water density and hence circulation are also modified by ventilation of the mixed layer through air–sea heat and freshwater fluxes. After the water mass is subducted into the interior ocean, its properties remain relatively unchanged as it circulates through the global ocean. The high-latitude formation of ocean bottom water is a critical component of the global ocean circulation. At high latitudes, surface cooling produces deeper mixing and ventilation. Salinity becomes a major factor controlling density where temperatures approach the freezing point. Thus, the analysis of high-latitude ocean processes depends on accurate surface heat and freshwater fluxes, including freshwater fluxes linked to ice formation, export, and melt. For example, buoyancy gain by excess precipitation and buoyancy loss by ocean heat loss are apparently of comparable importance in estimating Subantarctic Mode Water formation, which dominates the upper ocean just north of the Antarctic Circumpolar Current (Cerovecki et al. 2013). Calculation of surface water mass transformation rates from air–sea fluxes requires accurate and unbiased fluxes. Using the best available data products to evaluate the oceanic mixed-layer heat budget, Dong et al. (2007) found that the zonally averaged imbalance can be

products from numerical weather prediction (NWP) centers such as the European Centre for Medium-Range Weather Forecasts (ECMWF) and the National Centers for Environmental Prediction (NCEP). More numerous and more accurate in situ and satellite observations are required.

In view of the importance of high-latitude surface fluxes and the challenges in measuring them, it is reasonable to ask what accuracy is needed for different applications. "Examples: Surface fluxes from a climate research perspective" highlights a wide range of applications that makes use of surface flux observations. In Fig. 3, we summarize flux accuracy requirements that have emerged from discussions with researchers representing atmospheric science, oceanography, and Arctic sea ice physics. The

consensus is that the shortcomings in high-latitude observing systems and NWP are too great to allow for the determination of precise accuracy requirements for most processes. The values shown in Fig. 3 are therefore rough estimates to be refined as observing systems and NWP systems improve.

Climate processes occur on a suite of space and time scales with different accuracy requirements and challenges (Fig. 3). For measurements of smaller-scale processes (<100 km), for example, the barrier wind event embedded within a cold-air outbreak off the east coast of Greenland (see Fig. 4; Petersen and Renfrew 2009), in situ temperature, and wind speed are well sampled only at a few specific sites. Even at these measurement sites, observational error of turbulent fluxes is dominated by random errors. Note the

50 W m^{-2} and that locally, the upper-ocean heat balance can have an RMS misfit of more than 200 W m^{-2} at any given location, and 130 W m^{-2} in a global RMS-averaged sense. In order to discern the details of the upper-ocean heat storage and meridional overturning circulation, RMS errors must be substantially reduced, to 10 W m^{-2} or better for weekly to monthly time scales. Achieving such accuracy requires much better sampling and a reduction in biases: strong winter storms account for much of the evaporation (outside of western boundary currents; Scott 2011) but such storms reduce the capabilities of satellite observing systems.

From an atmospheric circulation perspective. Winter land surface flux anomalies can result in temporally and regionally differing energy input to atmospheric circulations. For example, turbulent energy fluxes resulting from the opening up of previously ice-covered areas of the Arctic are especially large in boreal winter, averaging O(50–70 W m^{-2}) (Alam and Curry 1997). These anomalies can drive a quasi-stationary wave response that can reinforce or attenuate climatological stationary waves propagating into the stratosphere, resulting in either a negative or a positive tropospheric annular mode response (e.g., Smith et al. 2011). When considering high-latitude surface fluxes due to

opening or closing of sea ice cover in particular, studies have shown that certain "hotspots" for turbulent heat flux anomalies exhibit significant feedback between atmospheric circulation patterns and modes of variability of sea ice. In the Northern Hemisphere, the Barents Sea is such a location for the North Atlantic Oscillation (e.g., Strong et al. 2009), the Bering Sea for the west Pacific pattern (e.g., Matthewman and Magnusdottir 2011). In the Southern Hemisphere, no single pattern dominates in atmospheric variability and its interaction with sea ice anomalies; rather, a superposition of the Pacific–South America pattern and a quasi-stationary zonal wave train dominate the atmospheric interaction with sea ice anomalies (e.g., Yuan and Li 2008; Matthewman and Magnusdottir 2012). The understanding, detection, and modeling of these feedbacks would be improved if heat fluxes were accurate to 10 W m^{-2} at 5–10-km spatial resolution and hourly time resolution. This would require much more frequent sampling from satellites, increased accuracy in mean values, and reduced random errors.

From a sea ice mass balance perspective. Arctic sea ice is a highly visible indicator of climate change. The range in recent and projected future ice extent and volume from different models remains large, reflected in the surface energy fluxes simulated both

for the observational era and for future scenarios. Models are sensitive to small perturbations in sea ice albedo (Bitz et al. 2006), and intermodel scatter in absorbed solar radiation, partly due to differences in the simulated surface albedo, is a particular concern (Holland et al. 2010). Air–sea heat fluxes can also play a role in determining ice thickness: Perovich et al. (2008) showed that solar heating of open water warms the upper ocean sufficiently to erode Arctic sea ice mass from below. Ultimately, reduced ice thicknesses feeds back onto ocean–atmosphere processes by changing the surface albedo as the ice becomes semitransparent (Brandt et al. 2005) as well as the conductive and turbulent heat fluxes and emitted (upward) surface longwave radiation through the ice.

The formation and presence of ice triggers a step function change in radiative, heat, momentum, and gas fluxes (e.g., Fig. 4). Ice formation and accumulation processes are complex, including snow refreezing (common in the Antarctic), vertical migration of frazil ice, and dissolution, erosion, and breakup processes. These processes occur on length scales too small to be detected remotely or modeled explicitly with current technology. As stable multiyear ice declines, annual ice processes and extent will dominate air–sea interaction and high-latitude fluxes.

inability of NWP models to represent small spatial scales, such as the jump in heat flux in Fig. 4; these small scales are often critical for processes occurring in the boundary between surface types. For large-scale processes, on the scale of zonally averaged monthly fluxes (Fig. 5), individual observations are averaged, which reduces random errors by a factor of the square root of the number of independent observations, meaning that random errors have
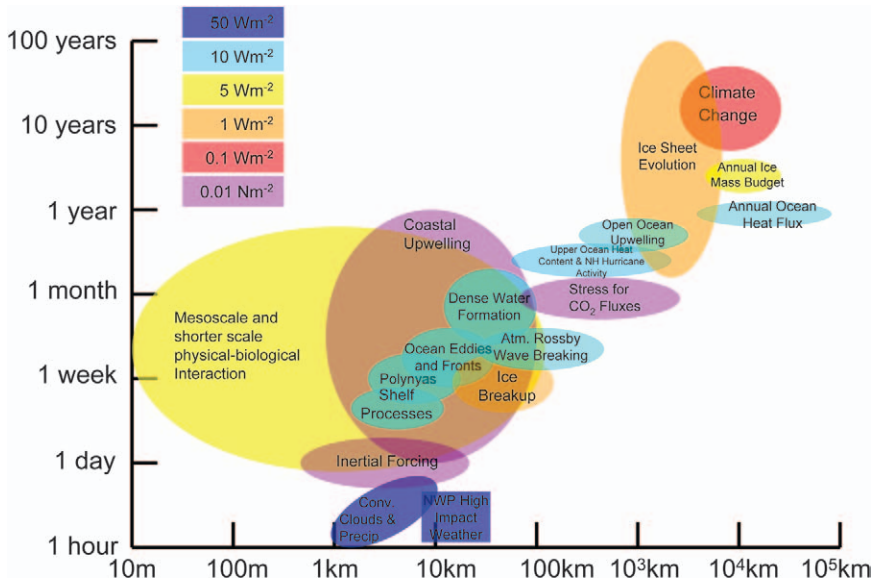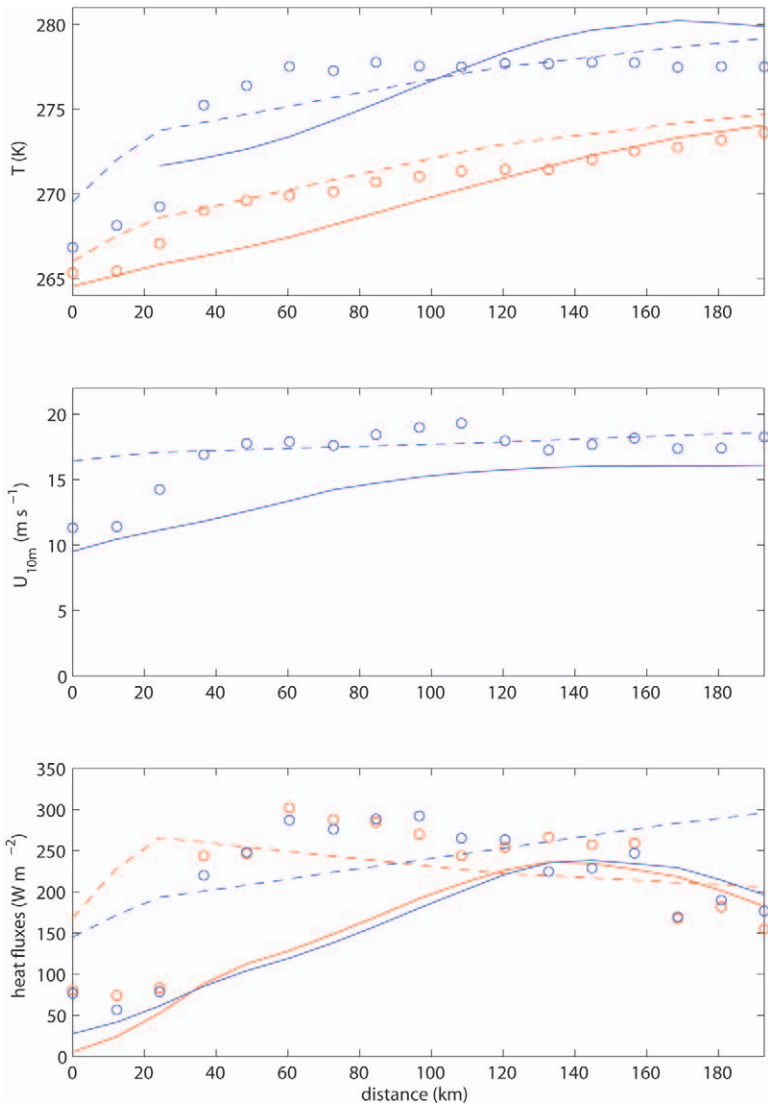
Fig. 3 (top). Spatial and temporal scales for high-latitude processes and the recommended accuracy of related surface fluxes. These accuracies are estimates from a wide range of scientists who require flux products for their research. The accuracy requirements are difficult to determine or validate as the modeling and observational errors—as well as the validity of assumptions—in current estimates are not sufficiently well understood to quantify requirements.

Fig. 4 (right). Boundary layer observations of a cold-air outbreak off the east coast of Greenland during an instrumented aircraft flight on 5 Mar 2007, as a function of distance from the coast. Shown are (top) 2-m temperature (red) and SST (blue), (middle) 10-m wind speed, and (bottom) surface SHFs (red) and LHFs (blue) calculated using the eddy covariance method (taken from Petersen and Renfrew 2009) as a function of distance. The observations are averaged into 12-km runs (circles). Interpolated estimates from ECMWF operational analyses (solid line) and the much coarser-resolution NCEP–National Center for Atmospheric Research Global Reanalysis 1 (NCEP-1, dashed line) are also plotted. The plots show a rapid warming from over the sea ice zone (0–30 km) off shore and a jump in wind speed and observed heat fluxes across the ice edge.

relatively little impact. Instead errors are dominated by biases in observations (which are typically small compared to random uncertainty in individual observations) or biases in parameterizations (e.g., Fig. 6). On the large scale, fluxes from NWP are typically limited by biases in parameterizations and related physical assumptions. Therefore, accurate individual observations or model simulations are needed to reduce the typically dominant sources of error for the smaller-scale processes, whereas dominant errors in larger-scale studies are reduced through low biases and accurate parameterizations. Importantly, some processes do not respond linearly to the forcing; for such processes, it is critically important to properly represent the distribution of fluxes, which are not well known (Monahan 2006, 2007; Gulev and Belyaev

2012). In current products these distributions differ enormously as demonstrated by the discrepancies in the median as well as in the 5th and 95th percentiles of sensible and latent heat flux (LHF) estimates shown in Fig. 5.

IMPROVING THE ACCURACY OF FLUXES.
The specific shortcomings in high-latitude surface fluxes result from a number of distinct issues. Here, we discuss problems stemming from flux parameterizations, observational errors, and sampling errors.

Flux parameterizations. Some flux estimates fail in part because they are calculated using parameterizations that have not been optimized for high-latitude conditions. Whereas surface turbulent fluxes can be
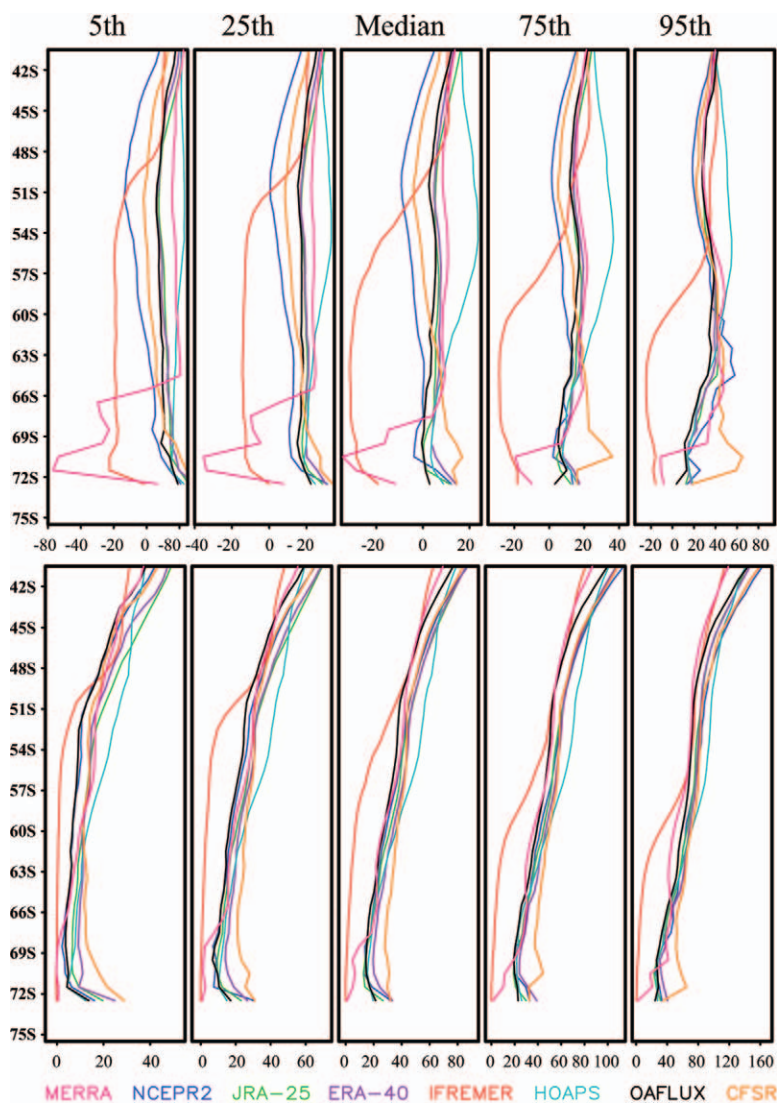

Fig. 5. Comparison of oceanic SHFs (top) and LHFs (bottom) in the Southern Ocean from readily available and sufficiently documented products: NCEP/Department of Energy Global Reanalysis 2 (NCEP-2, dark blue), Japanese Meteorological Agency (JMA, green), 40-yr ECMWF Re-Analysis (ERA-40, purple), L'Institut Français de Recherche pour l'Exploitation de la Mer (IFREMER, red), and Hamburg Ocean Atmosphere Parameters and Fluxes from Satellite Data (HOAPS, light blue), Woods Hole Oceanographic Institution objective analyzed air–sea fluxes (OAFlux, black), NCEP Climate Forecast System Reanalysis (CFSR, orange), and the National Aeronautics and Space Administration (NASA) Modern Era Retrospective-Analysis for Research and Applications (MERRA, magenta). Each box shows zonally averaged (0°–360°) monthly fluxes for the 5th, 25th, 50th, 75th, or 95th percentiles. The period for comparison (for which all products are available) is Mar 1992–Dec 2000. Clearly, there are very large differences in the distribution of fluxes. Note that the range of fluxes (x axis) is not constant, with the range for the 95th percentile being about 4 times the range for the 5th percentile. Furthermore, there is a great deal of regional surface flux variability in all high-latitude seas: product differences are greater on smaller spatial and temporal scales. Details about the first five products, parameterizations, and assumptions used to develop these products are given in Smith et al. (2010). The MERRA averages have unusual decreases in LHFs near the pole, which we believe is due to including ice-covered grid cells in the average (since the MERRA product does not have an ice mask).
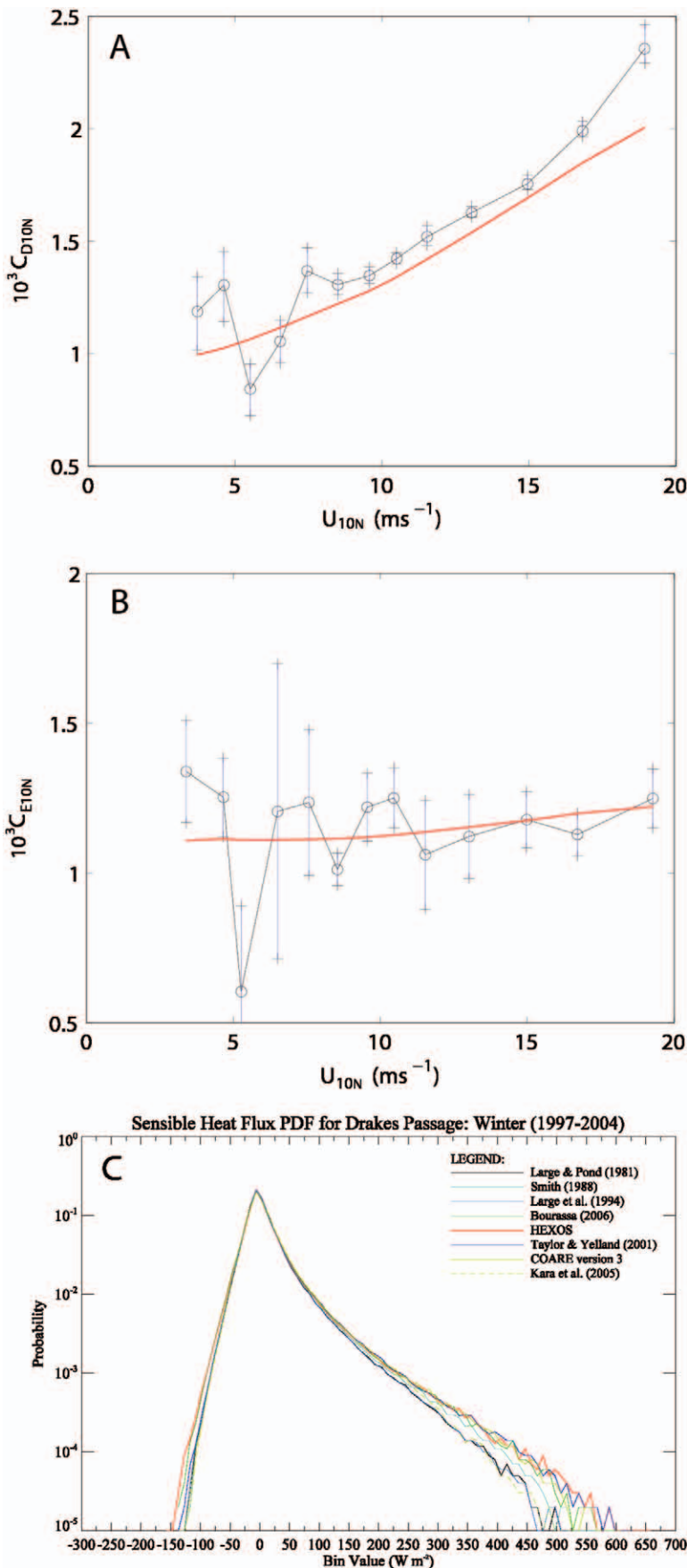
measured directly with specialized sensors placed on suitable platforms over the ocean (e.g., Wanninkhof et al. 2009; Ho et al. 2011), most applications require estimates distributed over a broader range in space and time than can be achieved with dedicated flux sensors. Thus, direct in situ flux observations are used to develop and tune indirect parameterizations, known as *bulk flux algorithms*, which allow fluxes to be calculated from more easily measured variables such as wind speed and sea surface temperature. Bulk flux algorithms have been in use for decades (see, e.g., Sverdrup 1937; Bunker 1976; Blanc 1985; Curry et al. 2004). Advances in understanding the physical processes involved in air–sea exchange and in observing technologies have promoted steady improvements in the sophistication and accuracy of these algorithms. Bulk flux algorithms are also used in retrievals of turbulent fluxes from satellite observations (Bourassa et al. 2010b). They have been used extensively to estimate the heat balance of the oceans from historic weather observations from volunteer observing ships [see Gulev and Taylor (2000) and references therein], and they form the basis for describing the atmosphere–ocean boundary interactions in virtually all climate and NWP models.

Fig. 6. Transfer coefficients for fluxes of (top) momentum and (middle) latent heat, based solely on high-latitude data, shown as a median (circle) and one standard deviation in the mean (error bars). These plots are based on data from only four regions: small departures from the global-mean dependencies (red line from COARE3.0 model) but not unreasonable because of the very small number of regions sampled. (bottom) The probability of distribution of SHFs in the area west of Drake Passage for winter (Jun–Jul) of 1997–2004 for different bulk parameterization algorithms applied to the same input data (Large and Yeager 2009).

There are two dominant sources of error in bulk algorithms—systematic errors in the transfer coefficient (including, e.g., structural errors in specifying the functional form of the parameterization) and the accuracy of the routinely observed variables (including not only measurement errors but also errors from transferring from NWP and satellite observations to real-world values, and errors due to mismatches in spatial and temporal scales)—used to compute the fluxes. The transfer coefficients are largely functions of wind speed (relative to the water surface) and air–sea temperature differences; C_D (Fig. 6a), C_E (Fig. 6b), and C_G are also a function of sea state. High-latitude estimates of transfer coefficients for momentum, sensible, or latent heat flux, and gas exchange are in reasonably good agreement for a wide range of ocean conditions (at least for 10-m wind speeds between 4 and 16 m s^{-1}, and for unstable through weakly stable stratification); however, there is considerable disagreement for lower and higher wind speeds. Observations are sparse in high latitudes, and wind and temperature conditions differ from those in midlatitudes. This results in large uncertainties in the transfer coefficients (Figs. 6a,b). However, most high wind speed observations are from high latitudes; therefore, they are a good match to the global values. An additional consideration is that there are few high-latitude studies, meaning that the observations come from only a few regions: these regions might not be representative of all high latitudes.

Available bulk parameterizations differ algorithmically and can produce different results, even given common input data: in Fig. 6c, sensible heat flux (SHF) probability densities are shown, computed from version 2 of the Common Ocean–Ice Reference Experiments (CORE; Large and Yeager 2009) data. For low wind speeds, parameterization differences cause only small changes in fluxes, and Fig. 6c shows the bulk parameterizations to be in good agreement when the sensible heat flux is between about −50 and +50 W m^{-2}. However, in high latitudes, the air–sea temperature difference can be large, implying large sensible heat fluxes, and in these conditions the bulk parameterizations do not agree well. In addition, bulk parameterization differences associated with waves and high wind speeds are also large. For example, one of the dominant

TABLE 1. Bulk formulas used to parameterize turbulent heat fluxes. The equations rely on differences between variables measured at known heights (e.g., 10 m) above the ocean surface (e.g., U_{10}) and those measured at the surface (e.g., U_s). Terms include the friction velocity u_*, which is a complicated function of the wind shear ($U_{10} - U_s$), waves, and the atmospheric stratification; air density (ρ); and air–sea differences in potential temperature ($\theta_{10} - \theta_s$), humidity ($q_{10} - q_s$), or gas concentration ($G_{s,aq} - G_{10}/H$). Here, θ_* and q_* are scaling parameters analogous to u_*, C_p is the specific heat of air, L_u is the latent heat of vaporization, and H is the Henry's law constant. The transfer coefficients—C_D, C_H, C_E, C_G—for momentum, specific heat, latent heat, and gas exchange, respectively, should account for subgrid-scale variability, and they can include additional dependence on wave steepness, wave age, u_*, and atmospheric stability (e.g., Yelland et al. 1998; Hwang 2005).

Momentum (wind stress)	$\tau = \rho u_*|u_*| = \rho C_D(U_{10} - U_s)|(U_{10} - U_s)|$
SHF	$Q_S = -\rho C_p \theta_*|u_*| = \rho C_p C_H(\theta_{10} - \theta_s)|(U_{10} - U_s)|$
Evaporation	$E = -\rho q_*|u_*| = \rho C_E(q_{10} - q_s)|(U_{10} - U_s)|$
LHF	$Q_L = -\rho L_v q_*|u_*| \approx L_v E$
Air–sea gas exchange	$F_G = C_G(G_{s,aq} - G_{10}/H)|(U_{10} - U_s)|$

reasons for the spread in Fig. 6c is that the parameterizations that do not consider sea state (Large and Pond 1981; Smith 1988; Large et al. 1994; Kara et al. 2005) locally have smaller fluxes than the parameterizations that consider waves [Humidity Exchange Over the Sea (HEXOS); Smith et al. 1992; Taylor and Yelland 2001; Coupled Ocean–Atmosphere Response Experiment version 3 (COARE3) using Taylor and Yelland's sea state; Fairall et al. 2003; Bourassa 2006].

In some cases, bulk parameterizations may simply be introducing an unnecessary layer of complication in the effort to determine surface fluxes. For example, since centimeter-scale radar backscatter is more closely tied to stress than to wind (Bourassa et al. 2010a), scatterometers can probably be tuned to measure stress and hence determine u_* (see Table 1) without the problems associated with the C_D dependence on sea state (e.g., Fairall et al. 1996; Bourassa 2006). Tuning stress retrievals and transfer coefficients for atypical conditions, or conditions that are adverse to in situ sensors, will be a challenge, given the paucity of observations and the importance of physical processes that are not yet well modeled in current parameterizations: for example, sea spray at high wind speeds (Andreas et al. 2008), rain (Weissman and Bourassa 2011), and mixed ice and water (Alam and Curry 1997). These conditions occur regularly in high latitudes and are linked to processes that are important to climate. Purely algorithmic differences (Fig. 6c) highlight how considering sea state can have a large impact on extreme fluxes in the Southern Ocean.

Different challenges arise for estimating radiative fluxes, which include shortwave (SW) radiation from the sun; SW reflected from the surface; and longwave (LW) radiation emitted from the land, ocean, ice, and atmosphere. Information on SW fluxes (SWFs) is obtained from ground measurements, numerical models, or as estimated from satellite observations using empirical, statistical, and/or physically based methods (Schmetz 1989, 1991, 1993; Pinker et al. 1995; Whitlock et al. 1995; Wielicki et al. 1995). The downward SW flux at the surface is the fraction of the SW flux received at the top of the atmosphere that is transmitted through the atmosphere. The transmittance depends on the composition of the atmosphere (e.g., amount of water vapor and ozone, optical thickness of cloud and aerosols) and on the path the radiation travels through the atmosphere. The upward SW flux at the surface is then determined by multiplying the surface downward flux by the surface albedo.

Uncertainties in the SW fluxes stem principally from uncertainty in cloud amount, and to a smaller degree from the uncertainties in the atmospheric clear-sky transmittance and in the surface albedo. Estimates of radiative fluxes from different satellite-based products disagree most in the polar regions during summer, as illustrated by the red line in Fig. 7, which shows comparatively large discrepancies between July shortwave fluxes poleward of 60°N. Estimates from the Surface Heat Budget of the Arctic Ocean (SHEBA) project and from high-latitude buoy and land stations suggest that satellite-based analyses provide downward shortwave radiative fluxes with residual bias on the order of 5 W m^{-2} and a standard deviation of 25 W m^{-2} on daily-averaged time scales (e.g., Perovich et al. 1999; Curry et al. 2002; Niu et al. 2010; Niu and Pinker 2011). Much of the standard deviation comes from comparing in situ point observations with satellite estimates representing larger spatial scales (e.g., pixel averages of 5 km × 5 km or larger areas).

Estimating LW surface radiative fluxes from satellites is also challenging. Downwelling LW surface radiation is controlled by the vertical profiles of temperature, gaseous absorbers, clouds, and aerosols. In contrast to the tropics, at high latitudes the moisture content of the atmosphere is low. As a result, the high-latitude atmosphere is semitransparent in some infrared bands that are normally opaque (Turner and Mlawer 2010), which increases the accuracy of surface and near-surface flux estimates. An especially formidable issue is that the LW flux (LWF) depends strongly on the cloud-base height (which only recently is becoming detectable from the A-Train

satellite constellation) and that quantities measured by satellite are not directly correlated to downwelling radiation. Consequently, downwelling LW is often estimated as a function of a bulk atmospheric temperature approximated by air temperature at the ground and an estimated broadband atmospheric emissivity. For cloudless skies, more than half the LW flux received at the ground comes from emissions in the lowest 100 m (Zhao et al. 1994), because the lowest atmospheric layers are relatively warmer and moister than higher layers and intercept some of the radiation emitted by higher layers. These factors contribute to particularly high uncertainty in downwelling LW at high latitudes: as the blue range bars in Fig. 7 indicate, discrepancies between different products for monthly-mean LW fluxes are larger poleward of about 65° latitude than they are in the tropics or midlatitudes.

Surface downward LW fluxes at high latitudes have not been evaluated over the ocean but have been evaluated against land-based observations (e.g., König-Langlo and Augstein 1994; Key et al. 1996; Guest 1998; Makshtas et al. 1999) and are typically accurate to ~10–30 W m^{-2} at high latitudes at monthly time scales (Perovich et al. 1999; Nussbaumer and Pinker 2012). For example, the parameterization of König-Langlo and Augstein (1994) reproduced the observations with root-mean-square (RMS) differences of <16 W m^{-2}. Though these accuracies are reasonable, like the SW flux accuracies, they are insufficient to meet the requirements indicated in Fig. 3 for many applications. For short time and small spatial scales, the largest sources of uncertainty in radiative fluxes are thought to stem from algorithm implementation problems associated with issues such as diurnal corrections and radiance-to-flux conversions (Wielicki et al. 1995).

For precipitation, oceanic in situ observations are extremely sparse and require dedicated support to maintain good accuracy (Bradley and Fairall 2006). Satellite retrievals are of poor quality over cloudy and snow- and ice-covered surfaces (e.g. Gruber and Levizzani 2008; Sapiano 2010), and it appears that better estimates can be obtained from atmospheric reanalyses (Serreze et al. 2005) or from combinations of satellite plus reanalysis and/or station data (Huffman et al. 1997; Xie and Arkin 1997). However, precipitation biases in reanalysis fields can be very large (Serreze and Hurst 2000), in part because of errors in radiative heating calculations and in part because of model microphysics and transport errors leading to incorrect input to the radiative transfer model. The proposed Polar Precipitation Mission

(PPM; Joe et al. 2010), an active 94-
and 35-GHz radar in a 400-km-high
polar orbit, is specifically designed to
fill these gaps and includes the capa-
bility to measure light snow falling
from shallow precipitation systems.

Observation error. Even if flux pa-
rameterizations were perfect, one
is still left with the problem of ob-
taining high-quality observations.
Observation error refers to error
characteristics of single observa-
tions or a derived quantity. For most
sensors and observations, these are
serious concerns. For example, gauge
errors in measured precipitation for
Arctic stations can exceed 100% in
winter (Yang 1999). Direct covari-
ance flux measurement systems have
a number of issues [see Fairall et al.
(2000) or Yelland et al. (2009) for a
discussion]. For quantities such as
latent heat or CO_2 fluxes, active or
periodic maintenance is required
to remove contamination of opti-
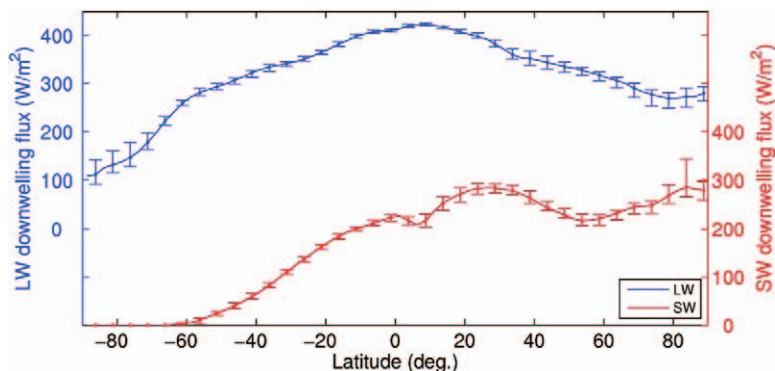cal surfaces and variable crosstalk
corrections (e.g., Prytherch et al.

Fɪɢ. 7. Zonal-mean all-sky surface downwelling SWFs and LWFs for Jul. The means (solid lines) show the ensemble monthly mean, averaged over available datasets. Error bars indicate the range of model means. SW datasets include University of Maryland (UMD)/DX version 3.3.3 (Ma and Pinker 2012) (at 0.5° scaled to 2.5°), UMD/Moderate Resolution Imaging Spectrometer (MODIS) (Wang and Pinker 2009) (at 1° scaled to 2.5°), Clouds and the Earth's Radiant Energy System (CERES)– Surface Radiation Budget Average (SRBAVG, 2.5°) (Wielicki et al. 1996), GEWEX version 3.0 (Stackhouse et al. 2011) (at 1° scaled to 2.5°), and International Satellite Cloud Climatology Project flux data (ISCCP-FD) (Zhang et al. 2004) (2.5°). The SW averaging period is Jul 2001–Jul 2007; MODIS was available only for Aug 2002–Aug 2008. LW models include UMD/ LW version 2.0 as implemented with MODIS data (1°) (Nussbaumer and Pinker 2012), ECMWF Interim Re-Analysis (ERA-Interim) (1.5°), GEWEX version 3.1 (1°), and ISCCP-FD (2.5°). The LW averaging period is Jul 2004–Jul 2007.

2010; Edson et al. 2011). Many ships and buoys have
well-maintained sensors and routinely report the
observations needed for input to bulk formulas with
sufficiently small random errors for many applica-
tions. However, substantial biases can occur because
of important metadata for observations collected
on ships, such as the physical height of sensors and
whether the anemometer at the time of observation is
on the leeward or windward side of the ship (Bradley
and Fairall 2006). Polar conditions are also very harsh
on instruments, which can necessitate special equip-
ment or frequent maintenance.

Satellite observations vary in reliability.
Scatterometer wind observations have consistent
accuracies for individual sensors but are not yet
intercalibrated, particularly for high wind speeds
(Bourassa et al. 2010c). Unfortunately, available scat-
terometers do not fully resolve the tight gradients
that occur along fronts and within strong extra-
tropical cyclones, nor do they provide the temporal
resolution needed to track rapidly evolving storms.
Moreover, since the demise of the Quick Scatterom-
eter (QuikSCAT) in November 2009, researchers
have relied more on the Advanced Scatterometer
(ASCAT), which is less affected by precipitation but

has a narrower swath than QuikSCAT, limiting the
view of large-scale storms. In addition, ASCAT is
currently calibrated differently than QuikSCAT for
10-m winds U_{10}, >15 m s^{-1}. For extreme winds found
in strong midlatitude cyclones, these difference can
exceed 10 m s^{-1} (Bourassa et al. 2010c).

Satellites can be quite effective for observing sea
surface temperatures (SSTs). Microwave sensors
perform well through cloudy conditions even in the
Southern Ocean (Dong et al. 2006), but infrared
sensors, which are required to resolve small-scale
features, are thwarted by clouds, resulting in little or
no high-resolution data in perennially cloudy regions,
such as parts of the Southern Ocean. Furthermore,
microwave satellite instruments are ineffective if
there is land or ice within the instrument footprint
(or even within the areas of relatively strong signal
outside the main footprint), and this excludes some
regions of great interest. The new generation of SST
products that optimally blend in situ, microwave, and
infrared observations might provide a way forward
(e.g., Donlon et al. 2007). Recent satellite observations
are improving estimates of surface albedo and aero-
sols (e.g., Schaaf et al. 2002; Remer et al. 2005; Kahn
et al. 2005), although the dominant observation error

source (sampling errors will be discussed in the next section) still stems from calibration uncertainties in satellite instruments. There are very large differences between estimates from NWP, satellites, and in situ products (Smith et al. 2010). Recent techniques for retrieving air temperature and humidity (Jackson et al. 2006, 2009; Jackson and Wick 2010; Roberts et al. 2010; Dong et al. 2010) have yielded improved estimates over a wider range of conditions. These retrievals have noise that is mildly worse than in situ observations; however, they have substantial biases over the very cold water that characterizes high latitudes. The impact of these improvements on turbulent fluxes remains to be determined (Bourassa et al. 2010b).

Some studies make use of NWP estimates of bulk variables (SST, air temperature, humidity, and other variables) to obtain surface fluxes through bulk parameterizations (e.g., Renfrew et al. 2002). These bulk variables and the resulting fluxes typically have large regional biases (Smith et al. 2010). In coupled climate models, biases both in the bulk variables and in the bulk flux parameterizations can introduce larger errors in the fluxes and feedbacks in the coupled systems. Typically, transfer coefficients in climate models have been modified to account for these biases. However, this type of tuning means that any modeled responses to changes in wind, temperature, and humidity are likely inaccurate, which is a serious problem in high latitudes, where several key climate processes (including ocean uptake of heat and water mass transformation) are sensitive to the magnitude of energy fluxes, and freshwater fluxes, and to the directional stress.

Improved observations of air–sea temperature differences and measurements of stress will improve the accuracy of CO_2 flux retrievals from satellites. The largest sources of error in CO_2 fluxes are insufficient sampling of the highly variable winds in polar latitudes, large changes in the partial pressure of CO_2 (pCO_2) across the air–sea interface in areas of differing biological activity (Martz et al. 2009), and indirect methods of regionally estimating oceanic pCO_2 from satellite observations (e.g., Sarma et al. 2006; Arrigo et al. 2010). These atmospheric and aqueous pCO_2 estimates require ongoing validation from observations collected by research vessels. Satellites currently lack the ability to measure atmospheric pCO_2 with sufficient accuracy at the desired resolution; however, lidar (Wilson et al. 2007) and the Atmospheric Infrared Sounder (AIRS; Engelen et al. 2004; Engelen and McNally 2005; Engelen and Stephens 2004; Strow and Hannon 2008) show promise for the future.

For radiative fluxes, observational errors are similarly important. Shi and Long (2004) discussed the accuracy limits of ground observations. Clouds are major modulators of the SW budgets, and aerosols (e.g., Arctic haze) are also important; however, information on their physical properties and vertical structure is not readily available, particularly in polar regions, in part because ice or snow and low clouds are difficult to distinguish in satellite data. Since satellites are critical for obtaining estimates of radiative fluxes on time and space scales that extend beyond the scope of field programs, one important step is to compare satellite-based downward surface flux estimates against ground measurements. At most latitude ranges, globally distributed ground measurements have improved over the last 12 years with the advent of the Global Energy and Water Cycle Experiment (GEWEX) Baseline Surface Radiation Network (Ohmura et al. 1998; Michalsky et al. 1999), with recent studies reporting satellites and ground stations agreeing within 10 W m^{-2} on a monthly time scale (e.g., Charlock and Alberta 1996; Zhang et al. 2004; Trenberth et al. 2009; Stackhouse et al. 2011; Ma and Pinker 2012; Nussbaumer and Pinker 2012). At high latitudes, satellite/ground station radiative flux comparisons show similar levels of agreement (Niu et al. 2010; Niu and Pinker 2011), but a more extensive network of high-latitude ground stations is needed.

Sampling error. The last major challenge for obtaining quality surface fluxes is sampling errors. This refers to error characteristics associated with undersampling natural variability. Important cases of undersampling also occur when observations are made conditionally, for example, only in clear or nonprecipitating conditions. Undersampling can result in large and non-Gaussian errors (Gulev et al. 2007a,b) and spatial/temporal inhomogeneity in error characteristics (Schlax et al. 2001; Hughes et al. 2012). Furthermore, scales smaller than the scale of the observation network can alias onto the larger scales that are resolved. High-latitude sampling errors are large because there are so few observations, and there are large changes in variables over relatively small times and distances. In situ radiative flux data for high latitudes come from land-based radiometer measurements, and there are relatively few in situ observations of SW or LW fluxes over high-latitude oceans. Flux moorings have not been deployed routinely in any high-latitude region. In situ ocean data that are available have hence been limited largely to collections from ships. In regions with major shipping routes, volunteer observing ships (VOSs)

now provide enough data to calculate surface energy fluxes, although monthly averages still have large errors (Berry and Kent 2011). However, south of 30°S and poleward of 50°N, there are few ship observations and large natural variability, and wind stress differences between VOSs and satellite products can be more than 3 times greater than differences observed elsewhere in the world (e.g., Risien and Chelton 2008). For studies of the upper-ocean heat content, profiling Argo floats have been a boon. However, Argo's target of sampling at 10-day temporal resolution and 3° spatial resolution precludes resolving details of spatial and temporal surface flux variations, and Argo floats do not normally make measurements in ice-covered areas. High-inclination polar-orbiting satellites have relatively good sampling in polar regions; however, the natural variability and covariability of winds, rain, and clouds is also quite large, resulting in large sampling errors. Thus, since cloud amount and type are tied to synoptic weather patterns, IR sensors in particular provide only conditional sampling of meteorological conditions.

In some cases relevant data, particularly those affecting radiative fluxes, are simply not part of the observational data stream. The high albedo of snow and ice, together with the cold and fairly dry atmosphere, results in a surface net radiation deficit for most months. Cloud cover typically reduces the radiation deficit (Pietroni et al. 2008) by absorbing upward LW and reemitting some of it back toward the surface. Thus, Pietroni et al. (2008) concluded that differences in LW distributions between two Antarctic sites, one near the coast and one in the interior, were strongly related to differences in cloud cover. Cloud-related scattering of SW is also unusually important in this region. However, the characteristics of clouds and aerosols in polar regions are poorly known and not routinely measured (Lubin and Vogelmann 2006).

Sampling problems are compounded by the fact that fluxes at high latitudes vary over shorter spatiotemporal scales than fluxes at lower latitudes. For surface turbulent fluxes, length scales over the high-latitude open ocean are determined by the first baroclinic Rossby radius, which can be 20 km or less (Chelton et al. 1998), and time scales can range from a couple of days to <6 h (e.g., Condron et al. 2008; Jiang et al. 2012), because high-latitude storms evolve quickly. Physics at meter to kilometer scales also matters: breaking waves and whitecaps are of first-order importance in production of sea spray (Andreas and Monahan 2000; Andreas and Emanuel 2001; Lewis and Schwartz 2004; Fairall et al. 2009) and hence in variations of albedo and surface

emissivity, in gas transfer (e.g., Woolf 2005), and of some importance in wind stress relationships (e.g, Mueller and Veron 2009).

Precipitation is notoriously difficult to determine. For example, Serreze et al. (2005) estimate that at a coarse gridcell resolution of 175 km, obtaining an accurate assessment of the monthly gridcell precipitation requires typically 3–5 stations within the cell—and more in topographically complex areas. However, for the Arctic terrestrial drainage, only 38% of the 175-km grid cells contain even a single station. The situation is much worse over Antarctica, the Southern Ocean, and the Arctic Ocean. Sampling from satellites can have large errors in these regions, because even though satellite orbits overlap at high latitudes, time intervals between observations are in many cases too large compared to the variability associated with storm systems. The Tropical Rainfall Measuring Mission (TRMM), the dedicated precipitation mission, does not reach high latitudes, and other satellite products show anomalously high variability poleward of 50° latitude and in ice-covered areas (Sapiano 2010). Furthermore, satellite observations with large footprints have insufficient spatial resolution to capture the spatial variability found in this typically inhomogeneous environment. Because precipitation rates are nonlinearly dependent on microwave emissions, patchy precipitation within the satellite footprint increases the bias and uncertainty of precipitation retrievals (North and Polyak 1996).

Ultimately, it is anticipated that NWP products with finer resolution and improved assimilation will help resolve the sampling problem. The higher-resolution fields released by ECMWF and other NWP producers in support of the Year of Tropical Convection (e.g., Waliser and Moncrieff 2008) are a first effort at this, but Jiang et al. (2012) found that even the newer reanalysis products did not resolve small-scale variations in Drake Passage turbulent heat fluxes. Routine, high-resolution NWP reanalyses with sufficient accuracy appear to be decades in the future and will require considerable development of the basic flux physics (or flux parameterizations) embedded in the model. We recommend further development of high-latitude reanalysis products, including the improvement of flux parameterizations, to address many of these difficulties. However, we note that efforts to advance reanalyses, refine parameterizations, and improve satellite products are all likely to require better data.

SUMMARY: KEY NEEDS. Obtaining improved estimates of high-latitude surface fluxes will require

a multifaceted effort. Coordinated sets of targeted observations are needed to refine flux parameterizations for high-latitude conditions and to provide calibration and validation data. Given the difficult working conditions at high latitudes and the vast region involved, satellites, numerical weather prediction models, and other products, including high-resolution reanalyses, will necessarily play a key role. The first high-resolution Arctic-specific reanalysis products are now being released for the time period from 2000-2011 (or 2012), as part of the Arctic System Reanalysis (ASR; Bromwich et al. 2010). This situation will likely require a multinational array of satellites designed to provide good temporal and spatial sampling, with carefully selected instrumentation, as well as improved retrieval techniques aimed at minimizing errors in stress, air temperature, humidity, precipitation, radiation, and cloud aerosol properties.

Our recommendation is for the development of an expanded high-latitude observational network that is sustained and optimized to improve physical parameterizations and to provide validation and calibration for satellite instruments and data assimilation systems. New Arctic and Antarctic reanalyses should be pursued, with goals of refining data retrieval algorithms and assessing different models for boundary layers and fluxes in the presence of ice. Improving surface flux estimates in high-latitude regions will require broad community involvement. Planning documents generated for International Polar Year (IPY) and post-IPY activities have begun to articulate priorities (e.g., Dickson 2006; Rintoul et al. 2010). Some key ideas for improving fluxes emerged from discussions at a March 2010 workshop jointly organized by SeaFlux and the U.S. CLIVAR High Latitude Surface Flux Working Group (summarized in "Recommendations for improving high-latitude fluxes"). As a follow up to the workshop and other post-IPY discussion, it is critical that the community continue to seek consensus for plans to improve high-latitude surface fluxes.

RECOMMENDATIONS FOR IMPROVING HIGH-LATITUDE FLUXES

The myriad of problems identified with high-latitude surface fluxes call for concerted efforts to identify pathways toward improvement. With this in mind, the U.S. CLIVAR High Latitude Surface Flux Working Group and the SeaFlux program together organized a workshop in Boulder, Colorado, for 17–19 March 2010 (Bourassa et al. 2010b; Gille et al. 2010). The workshop attracted approximately 70 participants and included time for open discussion about priority strategies for improving flux estimates. The issues summarized here represent topics for which community consensus seems clear.

1) Acquire more in situ observations. The dearth of observations in both high-wind open-ocean regimes and ice-covered regimes means that all additional flux-relevant data are desirable. This includes standard meteorological data needed to compute fluxes from bulk parameterizations [e.g., from the Shipboard Automated Meteorological and Oceanographic System (SAMOS) program] as well as direct flux observations. A network of moorings (such as the Southern Ocean Flux Station, deployed southwest of Tasmania in March 2010 as part of the Australian Integrated Marine Observing System; Trull et al. 2010) would be desirable for capturing year-round meteorological

variability at fixed positions. Having large numbers of independent samples is particularly important to reduce uncertainties in spatially and temporally averaged flux estimates and in tuning satellite observations. Given the pitfalls associated with existing bulk parameterizations, direct measurements of fluxes are critical. These are more likely to be successful by placing semiautonomous instrumentation that require only light maintenance on board research vessels, either during limited-duration process studies [such as was done during Southern Ocean Gas Exchange Experiment (GasEx); Ho et al. 2011] or as part of routine observations from research vessels operating in high latitudes (Yelland et al. 2009). Such a system has operated on the U.K. RRS *Discovery* and the Norwegian *Polarfront* (Yelland et al. 2009). The U.S. National Science Foundation (NSF)-sponsored Antarctic vessels or the National Oceanic and Atmospheric Administration (NOAA)-sponsored Arctic ships would be ideal platforms for similar systems. Aircraft observations are also important, particularly in marginal ice zones. Since some aircraft have had difficulties operating at low elevations in icy regimes, it is anticipated that unmanned aerial vehicles (UAVs) will have an important role in acquiring near-surface atmospheric measurements.

Limited-duration process studies play an important role, both in increasing the general inventory of observations and also, more importantly, in helping to improve our understanding of physical processes that govern fluxes. There is strong community consensus for an updated version of the SHEBA project and also for an Antarctic analog to SHEBA aimed at capturing differences between the sea ice zones of the Arctic (historically dominated by thick, multiyear ice) and the Antarctic (historically predominantly thinner first-year ice).

2) Develop improved satellite-flux-observing capabilities. Important as in situ measurements are, ultimately the adverse conditions of high-latitude oceans, the vast size of the regions that need to be observed, and the small spatial/temporal scales of the variability mean that we will need to rely on satellite data to obtain a complete picture of air–sea fluxes. Satellite sensors are now able to measure most of the relevant variables with some degree of accuracy, including ocean wind or wind stress (scatterometry), sea surface temperature (infrared or microwave radiometers), and near-surface air temperature and humidity [atmospheric profiles such as the Advanced Microwave Sounding

REFERENCES

Alam, A., and J. A. Curry, 1997: Determination of surface turbulent fluxes over leads in Arctic sea ice. *J. Geophys. Res.,* **102** (C2), 3331–3344.

AMAP, 2011: AMAP Assessment 2011: Mercury in the Arctic. Arctic Monitoring and Assessment Programme, 193 pp. [Available online at www.amap.no /assessment/scientificbackground.htm.]

Andreas, E. L., and E. C. Monahan, 2000: The role of whitecap bubbles in air–sea heat and moisture exchange. *J. Phys. Oceanogr.,* **30,** 433–442.

——, and K. A. Emanuel, 2001: Effects of sea spray on tropical cyclone intensity. *J. Atmos. Sci.,* **58,** 3741–3751.

——, P. O. G. Persson, and J. E. Hare, 2008: A bulk turbulent air–sea flux algorithm for high-wind, spray conditions. *J. Phys. Oceanogr.,* **38,** 1581–1596.

Arrigo, K. R., S. Pabi, G. L. van Dijken, and W. Maslowski, 2010: Air–sea flux of CO_2 in the Arctic

Unit (AMSU) and AIRS]. Current work focuses on developing improved retrieval algorithms that push the limits of flux estimation using existing instruments. Ultimately, there is broad interest in developing a coordinated system of satellite instruments for heat and momentum fluxes. These could fly either on board a single satellite or on multiple satellites flying in formation as a "flux train," analogous to the current series of atmospheric satellites known as the A-Train. For time scales typical of the synoptic scale in the atmosphere, an accuracy of 5 W m^{-2} in net energy fluxes is considered a desirable, albeit challenging, target for the combined satellite and in situ observing system. Additional preliminary work will need to be completed to determine the extent to which this is possible with current satellite technology.

3) Make observations and flux products more accessible. Along with the need for more observations of high-latitude fluxes comes a parallel need to improve access to observations and the flux products derived from them (such as NWP reanalyses). This involves a number of issues that will benefit a broad range of user communities. Workshop participants noted that data users sometimes select flux-related data products primarily on the basis of the period covered, the specific variables available, or even the convenience of finding data, without considering the appropriateness of the dataset for a particular application. To address these existing difficulties, first, flux-related data need to be easy to find. Although high-latitude data are sparse, meteorological sensors have been installed on the Antarctic support vessels in recent years, and a number of recent programs have collected observations in adverse high-latitude conditions. Flux-related measurements from field programs, ships of opportunity, and satellites need to be archived. Data collectors and product developers are encouraged to provide their data to centers, where users can easily identify and cross compare a wide range of measurements and/or flux products that may be relevant for their work. More importantly, data providers and data centers need to release flux-relevant data along with a full set of metadata explaining the origins of the data and the inherent uncertainties.

4) Encourage flux intercomparison. Users of flux products often struggle to select a single flux product from among the plethora of options derived using different methods, all with different strengths and deficiencies. Given the lack of clear community consensus about how best to determine fluxes, a better approach is to intercompare multiple products (e.g., Dong et al. 2007; Cerovecki et al. 2011). Data providers in particular recommended that users take time to evaluate multiple flux products and to consider whether a specific flux product is suited for various applications. In a multiproduct approach, the variability among different products can sometimes serve as a crude measure of the robustness of results (cf. Fig. 5). While workshop participants suggested that a multiproduct approach is nearly always appropriate, they were also enthusiastic about establishing an organized effort to coordinate flux product intercomparisons and synthesize the results. For example, one suggestion was to develop a specific set of metrics (e.g., determining the effective resolution, biases, and uncertainties) and techniques (e.g., power density spectra) for evaluating flux data products that could be disseminated along with the data themselves. A step beyond establishing metrics for flux evaluation would be a global effort to improve the utility and interoperability of surface flux estimates analogous to the effort of the Group for High Resolution Sea Surface Temperature (GHRSST).

Ocean, 1998–2003. *J. Geophys. Res.,* **115**, G04024, doi:10.1029/2009JG001224.

Berry, D. I., and E. C. Kent, 2011: Air–sea fluxes from ICOADS: The construction of a new gridded dataset with uncertainty estimates. *Int. J. Climatol.,* **31,** 987–1001, doi:10.1002/joc.2059.

Bindoff, N., and Coauthors, 2007: Observations: Oceanic climate change and sea level. *Climate Change 2007: The Physical Science Basis,* S. Solomon et al., Eds., Cambridge University Press, 385–432.

Bitz, C. M., P. R. Gent, R. A. Woodgate, M. M. Holland, and R. Lindsay, 2006: The influence of sea ice on ocean heat uptake in response to increasing CO_2. *J. Climate,* **19,** 2437–2450.

Blanc, T. V., 1985: Variation of bulk-derived surface flux, stability, and roughness results due to the use of different transfer coefficient schemes. *J. Phys. Oceanogr.,* **15,** 650–669.

Bourassa, M. A., 2006: Satellite-based observations of surface turbulent stress during severe weather. *Atmosphere-Ocean Interactions: Volume 2,* W. Perrie, Ed., Advances in Fluid Mechanics, Vol. 39, Wessex Institute of Technology Press, 35–52.

——, E. Rodriguez, and R. Gaston, 2010a: NASA's Ocean Vector Winds Science Team workshops. *Bull. Amer. Meteor. Soc.,* **91,** 925–928.

——, S. Gille, D. L. Jackson, B. J. Roberts, and G. A. Wick, 2010b: Ocean winds and turbulent air-sea fluxes inferred from remote sensing. *Oceanography,* **23**, 36–51, doi:10.5670/oceanog.2010.04.

——, and Coauthors, 2010c: Remotely sensed winds and wind stresses for marine forecasting and ocean modeling. *Proceedings of the OceanObs'09: Sustained Ocean Observations and Information for Society Conference,* J. Hall, D. E. Harrison, and D. Stammer, Eds., Vol. 2, ESA Publ. WPP-306, doi:10.5270/OceanObs09.cwp.08.

Boyer, T. P., S. Levitus, J. I. Antonov, R. A. Locarnini, and H. E. Garcia, 2005: Linear trends in salinity for the World Ocean, 1955–1998. *Geophys. Res. Lett.,* **32,** L01604, doi:10.1029/2004GL021791.

——, ——, ——, ——, A. Mishonov, H. E. Garcia, and S. A. Josey, 2007: Changes in freshwater content in the North Atlantic Ocean 1955–2006. *Geophys. Res. Lett.,* **34,** L16603, doi:10.1029/2007GL030126.

Bradley, F., and C. Fairall, 2006: A guide to making climate quality meteorological and flux measurements at sea. NOAA Tech. Memo. OAR PSD-311, 109 pp.

Brandt, R. E., S. G. Warren, A. P. Worby, and T. C. Grenfell, 2005: Surface albedo of the Antarctic sea ice zone. *J. Climate,* **18,** 3606–3622.

Bromwich, D., Y.-H. Kuo, M. Serreze, J. Walsh, L.-S. Bai, M. Barlage, K. Hines, and A. Slater, 2010:

Arctic system reanalysis: Call for community involvement. *Eos, Trans. Amer. Geophys. Union,* **91,** doi:10.1029/2010EO020001.

Bunker, A. F., 1976: Computations of surface energy flux and annual air–sea interaction cycles of the North Atlantic Ocean. *Mon. Wea. Rev.,* **104,** 1122–1140.

Cerovecki, I., L. D. Talley, and M. R. Mazloff, 2011: A comparison of Southern Ocean air–sea buoyancy flux from an ocean state estimate with five other products. *J. Climate,* **24,** 6283–6306.

——, ——, ——, and G. Maze, 2013: Subantarctic Mode Water formation, destruction, and export in the eddy-permitting Southern Ocean state estimate. *J. Phys. Oceanogr.,* in press.

Charlock, T. P., and T. L. Alberta, 1996: The CERES/ARM/GEWEX Experiment (CAGEX) for the retrieval of radiative fluxes with satellite data. *Bull. Amer. Meteor. Soc.,* **77,** 2673–2683.

Chelton, D. B., R. A. de Szoeke, M. G. Schlax, K. El Naggar, and N. Siwertz, 1998: Geographical variability of the first baroclinic Rossby radius of deformation. *J. Phys. Oceanogr.,* **28,** 433–460.

Christensen, J. H., and Coauthors, 2007: Regional climate projections. *Climate Change 2007: The Physical Science Basis,* S. Solomon et al., Eds., Cambridge University Press, 847–940.

Comiso, J. C., C. L. Parkinson, R. Gersten, and L. Stock, 2008: Accelerated decline in the Arctic sea ice cover. *Geophys. Res. Lett.,* **35,** L01703, doi:10.1029/2007GL031972.

Condron, A., G. R. Bigg, and I. A. Renfrew, 2008: Modeling the impact of polar mesocyclones on ocean circulation. *J. Geophys. Res.,* **113,** C10005, doi:10.1029/2007JC004599.

Curry, J. A., J. L. Schramm, A. Alam, R. Reeder, T. E. Arbetter, and P. Guest, 2002: Evaluation of data sets used to force sea ice models in the Arctic Ocean. *J. Geophys. Res.,* **107,** 8027, doi:10.1029/2000JC000466.

——, and Coauthors, 2004: SeaFlux. *Bull. Amer. Meteor. Soc.,* **85,** 409–424.

Curry, R., and C. Mauritzen, 2005: Dilution of the northern North Atlantic Ocean in recent decades. *Science,* **308,** 1772–1774.

Dickson, B., 2006: The integrated Arctic Ocean Observing System (iAOOS): An AOSB-CliC Observing Plan for the International Polar Year. *Oceanologia,* **48,** 5–21.

Domingues, C. M., J. A. Church, N. J. White, P. J. Gleckler, S. E. Wijffels, P. M. Barker, and J. R. Dunn, 2008: Improved estimates of upper-ocean warming and multi-decadal sea-level rise. *Nature,* **453,** 1090–1096.

Dong, S., S. T. Gille, J. Sprintall, and C. Gentemann, 2006: Validation of the Advanced Microwave Scanning Radiometer for the Earth Observing

System (AMSR-E) sea surface temperature in the Southern Ocean. *J. Geophys. Res.,* **111,** C04002, doi:10.1029/2005JC002934.

——, ——, and ——, 2007: An assessment of the Southern Ocean mixed-layer heat budget. *J. Climate,* **20,** 4425–4442.

——, ——, ——, and E. J. Fetzer, 2010: Assessing the potential of the Atmospheric Infrared Sounder (AIRS) surface temperature and specific humidity in turbulent heat flux estimates in the Southern Ocean. *J. Geophys. Res.,* **115,** C05013, doi:10.1029/2009JC005542.

Donlon, C., and Coauthors, 2007: The Global Ocean Data Assimilation Experiment High-Resolution Sea Surface Temperature Pilot Project. *Bull. Amer. Meteor. Soc.,* **88,** 1197–1213.

Durack, P. J., and S. E. Wijffels, 2010: Fifty-year trends in global ocean salinities and their relationship to broad-scale warming. *J. Climate,* **23,** 4342–4362.

Edson, J. B., and Coauthors, 2011: Direct covariance measurement of CO_2 gas transfer velocity during the 2008 Southern Ocean Gas Exchange Experiment: Wind speed dependency. *J. Geophys. Res.,* **116,** C00F10, doi:10.1029/2011JC007022.

Engelen, R. J., and G. L. Stephens, 2004: Information content of infrared satellite sounding measurements with respect to CO_2. *J. Appl. Meteor.,* **43,** 373–378.

——, and A. P. McNally, 2005: Estimating atmospheric CO_2 from advanced infrared satellite radiances within an operational four-dimensional variational (4D-Var) data assimilation system: Results and validation. *J. Geophys. Res.,* **110,** D18305, doi:10.1029/2005JD005982.

——, E. Andersson, F. Chevallier, A. Hollingsworth, M. Matricardi, A. P. McNally, J.-N. Thépaut, and P. D. Watts, 2004: Estimating atmospheric CO_2 from advanced infrared satellite radiances within an operational 4D-Var data assimilation system: Methodology and first results. *J. Geophys. Res.,* **109,** D19309, doi:10.1029/2004JD004777.

Fairall, C. W., E. F. Bradley, D. P. Rogers, J. B. Edson, and G. S. Young, 1996: Bulk parameterization of air-sea fluxes for Tropical Ocean-Global Atmosphere Coupled-Ocean Atmosphere Response Experiment. *J. Geophys. Res.,* **101** (C2), 3747–3767.

——, J. E. Hare, J. B. Edson, and W. McGillis, 2000: Parameterization and measurement of air-sea gas transfer. *Bound.-Layer Meteor.,* **96,** 63–105.

——, E. F. Bradley, J. E. Hare, A. A. Grachev, and J. B. Edson, 2003: Bulk parameterizations of air–sea fluxes: Updates and verification for the COARE algorithm. *J. Climate,* **16,** 571–591.

——, M. L. Banner, W. L. Peirson, W. Asher, and R. P. Morison, 2009: Investigation of the physical scaling of sea spray spume droplet production. *J. Geophys., Res.,* **114,** C10001, doi:10.1029/2008JC004918.

Gille, S. T., 2002: Warming of the Southern Ocean since the 1950s. *Science,* **295,** 1275–1277.

——, M. A. Bourassa, and C. A. Clayson, 2010: Improving observations of high-latitude fluxes between atmosphere, ocean, and ice: Surface fluxes: Challenges at high latitudes; Boulder, Colorado, 17–19 March 2010. *Eos, Trans. Amer. Geophys. Union,* **91,** doi:10.1029/2010EO350003.

Gruber, A., and V. Levizzani, 2008: Assessment of global precipitation products: A project of the World Climate Research Programme Global Energy and Water Cycle Experiment (GEWEX) Radiation Panel. WCRP-128, WMO/TD-1430, 57 pp.

Guest, P. S., 1998: Surface longwave radiation conditions in the eastern Weddell Sea during winter. *J. Geophys. Res.,* **103** (C13), 30761–30771.

Gulev, S. K., and P. K. Taylor, Eds., 2000: Intercomparison and validation of ocean–atmosphere energy flux fields. WCRP-112, WMO/TD-1036, 303 pp.

——, and K. P. Belyaev, 2012: Probability distribution characteristics for surface air–sea turbulent heat fluxes over the global ocean. *J. Climate,* **25,** 184–206.

——, T. Jung, and E. Ruprecht, 2007a: Estimation of the impact of sampling errors in the VOS observations on air–sea fluxes. Part I: Uncertainties in climate means. *J. Climate,* **20,** 279–301.

——, ——, and ——, 2007b: Estimation of the impact of sampling errors in the VOS observations on air–sea fluxes. Part II: Impact on trends and interannual variability. *J. Climate,* **20,** 302–315.

Hansen, J., and Coauthors, 2005: Earth's energy imbalance: Confirmation and implications. *Science,* **308,** doi:10.1126/science.1110252.

Ho, D. T., and Coauthors, 2011: Southern Ocean Gas Exchange Experiment: Setting the stage. *J. Geophys. Res.,* **116,** C00F08, doi:10.1029/2010JC006852.

Holland, M. M., M. C. Serreze, and J. Stroeve, 2010: The sea ice mass budget of the Arctic and its future change as simulated by coupled climate models. *Climate Dyn.,* **34,** 185–200, doi:10.1007/s00382-008-0493-4.

Hosoda, S., T. Suga, N. Shikama, and K. Mizuno, 2009: Global surface layer salinity change detected by Argo and its implication for hydrological cycle intensification. *J. Oceanogr.,* **65,** 579–586.

Huffman, G. J. and Coauthors, 1997: The Global Precipitation Climatology Project (GPCP) combined precipitation dataset. *Bull. Amer. Meteor. Soc.,* **78,** 5–20.

Hughes, P., and M. A. Bourassa, J. Rolph, and S. R. Smith, 2012: Averaging-Related Biases in Monthly Latent Heat Fluxes. *J. Atmos. Oceanic. Technol.,* **29,** 974–986, doi:10.1175/JTECH-D-11-00184.1.

Hwang, P. A., 2005: Temporal and spatial variation of the drag coefficient of a developing sea under steady wind-forcing. *J. Geophys. Res.,* **110,** C07024, doi:10.1029/2005JC002912.

Jackson, D. L., and G. A. Wick, 2010: Near-surface air temperature retrieval derived from AMSU-A and sea surface temperature observations. *J. Atmos. Oceanic Technol.,* **27,** 1769–1776.

——, ——, and J. J. Bates, 2006: Near-surface retrieval of air temperature and specific humidity using multisensor microwave satellite observations. *J. Geophys. Res.,* **111,** D10306, doi:10.1029/2005JD006431.

——, ——, and F. R. Robertson, 2009: Improved multisensor approach to satellite-retrieved near-surface specific humidity observations. *J. Geophys. Res.,* **114,** D16303, doi:10.1029/2008JD011341.

Jiang, C., S. T. Gille, J. Sprintall, K. Yoshimura, and M. Kanamitsu, 2012: Spatial variation in turbulent heat fluxes in Drake Passage. *J. Climate,* **25,** 1470–1488.

Joe, P., and Coauthors, 2010: The Polar Precipitation Measurement Mission. *Proc. Sixth European Conf. on Radar in Meteorology and Hydrology,* Sibiu, Romania, European Meteorological Society, 18 pp. [Available online at www.erad2010.org/pdf/oral/tuesday/satellite/01_ERAD2010_Joe.pdf.]

Kahn, R. A., B. J. Gaitley, J. V. Martonchik, D. J. Diner, K. A. Crean, and B. Holben, 2005: Multiangle Imaging Spectroradiometer (MISR) global aerosol optical depth validation based on 2 years of coincident Aerosol Robotic Network (AERONET) observations. *J. Geophys. Res.,* **110,** D10S04, doi:10.1029/2004JD004706.

Kara, A. B., H. E. Hurlburt, and A. J. Wallcraft, 2005: Stability-dependent exchange coefficients for air–sea fluxes. *J. Atmos. Oceanic Technol.,* **22,** 1080–1094.

Karcher, M. J., R. Gerdes, F. Kauke, and C. Köberle, 2003: Arctic warming: Evolution and spreading of the 1990s warm event in the Nordic seas and the Arctic Ocean. *J. Geophys. Res.,* **108,** 3034, doi:10.1029/2001JC001265.

Key, J. R., R. A. Silcox, and R. S. Stone, 1996: Evaluation of surface radiative flux parameterizations for use in sea ice models. *J. Geophys. Res.,* **101** (C2), 3839–3849.

König-Langlo, G., and E. Augstein, 1994: Parameterization of the downward long-wave radiation at the Earth's surface in polar regions. *Meteor. Z.,* **3,** 343–347.

Kwok, R., and N. Untersteiner, 2011: The thinning of Arctic sea ice. *Phys. Today,* **64,** 36–41.

Large, W. G., and S. Pond, 1981: Open ocean momentum flux measurements in moderate to strong winds. *J. Phys. Oceanogr.,* **11,** 324–336.

——, and S. G. Yeager, 2009: The global climatology of an interannually varying air–sea flux data set. *Climate Dyn.,* **33,** 341–364.

——, J. C. McWilliams, and S. C. Doney, 1994: Oceanic vertical mixing: A review and a model with nonlocal boundary layer parameterization. *Rev. Geophys.,* **32,** 363–403.

Levitus, S., J. I. Antonov, and T. Boyer, 2005: Warming of the World Ocean, 1955–2003. *Geophys. Res. Lett.,* **32,** L02604, doi:10.1029/2004GL021592.

——, ——, ——, R. A. Locarnini, H. E. Garcia, and A. V. Mishonov, 2009: Global ocean heat content 1955–2008 in light of recently revealed instrumentation problems. *Geophys. Res. Lett.,* **36,** L07608, doi:10.1029/2008GL037155.

Lewis, E. R., and E. W. Schwartz, 2004: *Sea Salt Aerosol Production: Mechanisms, Methods, Measurements and Models—A Critical Review. Geophys. Monogr.,* Vol. 152, Amer. Geophys. Union, 413 pp.

Lubin, D., and A. M. Vogelmann, 2006: A climatologically significant aerosol longwave indirect effect in the Arctic. *Nature,* **439,** 453–456.

Ma, Y., and R. T. Pinker, 2012: Modeling shortwave radiative fluxes from satellites. *J. Geophys. Res.,* **117,** D23202, doi:10.1029/2012JD018332.

Makshtas, A. P., E. L. Andreas, P. N. Svyashchennikov, and V. F. Timachev, 1999: Accounting for clouds in sea ice models. *Atmos. Res.,* **52,** 77–113.

Martz, T. R., M. D. DeGrandpre, P. G. Strutton, W. R. McGillis, and W. M. Drennan, 2009: Sea surface $p\mathrm{CO_2}$ and carbon export during the Labrador Sea spring-summer bloom: An in situ mass balance approach. *J. Geophys. Res.,* **114,** C09008, doi:10.1029/2008JC005060.

Matthewman, N. J., and G. Magnusdottir, 2011: Observed interaction between Pacific sea ice anomalies and the western Pacific pattern on intraseasonal time scales. *J. Climate,* **24,** 5031–5042.

——, and ——, 2012: Clarifying ambiguity in intraseasonal Southern Hemisphere climate modes during austral winter. *J. Geophys. Res.,* **117,** D03105, doi:10.1029/2011JD016707.

Michalsky, J., E. Dutton, M. Rubes, D. Nelson, T. Stoffel, M. Wesley, M. Splitt, and J. DeLuisi, 1999: Optimal measurement of surface shortwave irradiance using current instrumentation. *J. Atmos. Oceanic Technol.,* **16,** 55–69.

Monahan, A. H., 2006: The probability distribution of sea surface wind speeds. Part II: Dataset intercomparison and seasonal variability. *J. Climate,* **19,** 521–534.

——, 2007: Empirical models of the probability distribution of sea surface wind speeds. *J. Climate,* **20,** 5798–5814.

Moore, G. W. K., R. S. Pickart, and I. A. Renfrew, 2008: Buoy observations from the windiest location in the World Ocean, Cape Farewell, Greenland. *Geophys. Res. Lett.,* **35,** L18802, doi:10.1029/2008GL034845.

Mueller, J., and F. Veron, 2009: A nonlinear formulation of the bulk surface stress over the ocean through a simple feedback mechanism. *Bound.-Layer Meteor.,* **130,** 117–134.

Niu, X., and R. T. Pinker, 2011: Radiative fluxes at Barrow, Alaska: A satellite view. *J. Climate,* **24,** 5494–5505.

——, ——, and M. F. Cronin, 2010: Radiative fluxes at high latitudes. *Geophys. Res. Lett.,* **37,** L20811, doi:10.1029/2010GL044606.

North, G. R., and I. Polyak, 1996: Spatial correlation of beam-filling error in microwave rain-rate retrievals. *J. Atmos. Oceanic Technol.,* **13,** 1101–1106.

Nussbaumer, E. A., and R. T. Pinker, 2012: Estimating surface longwave radiative fluxes from satellites utilizing artificial neural networks. *J. Geophys. Res.,* **117,** D07209, doi:10.1029/2011JD017141.

Ohmura, A., and Coauthors, 1998: Baseline Surface Radiation Network (BSRN/WRMC): New precision radiometry for climate research. *Bull. Amer. Meteor. Soc.,* **79,** 2115–2136.

Perovich, D. K., and Coauthors, 1999: Year on ice gives climate insights. *Eos, Trans. Amer. Geophys. Union,* **80,** doi:10.1029/EO080i041p00481-01.

——, J. A. Richter-Menge, K. F. Jones, and B. Light, 2008: Sunlight, water, and ice: Extreme Arctic sea ice melt during the summer of 2007. *Geophys. Res. Lett.,* **35,** L11501, doi:10.1029/2008GL034007.

Petersen, G. N., and I. A. Renfrew, 2009: Aircraft-based observations of air-sea fluxes over Denmark Strait and the Irminger Sea during high wind speed conditions. *Quart. J. Roy. Meteor. Soc.,* **135,** 2030–2045.

Petty, G. W., 2006: *A First Course in Atmospheric Radiation.* 2nd ed. Sundog Publishing, 472 pp.

Pietroni, I., P. Anderson, S. Argentini, and J. King, 2008: Long wave radiation behaviour at Halley and Concordia stations, Antarctica. *Geophysical Research Abstracts,* Vol. 10, Abstract EGU2008-A-03254. [Available online at http://meetings.copernicus. org/www.cosis.net/abstracts/EGU2008/03254 /EGU2008-A-03254.pdf.]

Pinker, R. T., R. Frouin, and Z. Li, 1995: A review of satellite methods to derive surface shortwave irradiance. *Remote Sens. Environ.,* **51,** 108–124.

Prytherch, J., M. J. Yelland, R. W. Pascal, B. I. Moat, I. Skjelvan, and C. C. Neill, 2010: Direct measurements of the CO_2 flux over the ocean: Development of a novel method. *Geophys. Res. Lett.,* **37,** L03607, doi:10.1029/2009GL041482.

Purkey, S. G., and G. C. Johnson, 2010: Warming of global abyssal and deep Southern Ocean waters between the 1990s and 2000s: Contributions to global heat and sea level rise budgets. *J. Climate,* **23,** 6336–6351.

Randall, D. A., and Coauthors, 2007: Climate models and their evaluation. *Climate Change 2007: The Physical Science Basis,* S. Solomon et al., Eds., Cambridge University Press, 589–662.

Remer, L. A., and Coauthors, 2005: The MODIS aerosol algorithm, products, and validation. *J. Atmos. Sci.,* **62,** 947–973.

Renfrew, I. A., G. W. K. Moore, P. S. Guest, and K. Bumke, 2002: A comparison of surface layer and surface turbulent flux observations over the Labrador Sea with ECMWF analyses and NCEP reanalyses. *J. Phys. Oceanogr.,* **32,** 383–400.

——, and Coauthors, 2008: The Greenland Flow Distortion Experiment. *Bull. Amer. Meteor. Soc.,* **89,** 1307–1324.

Rignot, E., G. Casassa, P. Gogineni, W. Krabill, A. Rivera, and R. Thomas, 2004: Accelerated ice discharge from the Antarctic Peninsula following the collapse of Larsen B ice shelf. *Geophys. Res. Lett.,* **31,** L18401, doi:10.1029/2004GL020697.

Rintoul, S. R., and Coauthors, 2010: Southern Ocean Observing System (SOOS): Rationale and strategy for sustained observations of the Southern Ocean. *Proceedings of OceanObs'09: Sustained Ocean Observations and Information for Society Conf.,* J. Hall, D. E. Harrison, and D. Stammer, Eds., Vol. 2, ESA Publ. WPP-306, doi:10.5270/OceanObs09.cwp.74.

Risien, C. M., and D. B. Chelton, 2008: A global climatology of surface wind and wind stress fields from eight years of QuikSCAT scatterometer data. *J. Phys. Oceanogr.,* **38,** 2379–2413.

Roberts, J. B., C. A. Clayson, F. R. Robertson, and D. L. Jackson, 2010: Predicting near-surface atmospheric variables from Special Sensor Microwave/ Imager using neural networks with a first-guess approach. *J. Geophys. Res.,* **115,** D19113, doi:10.1029/2009JD013099.

Sapiano, M. R. P., 2010: An evaluation of high resolution precipitation products at low resolution. *Int. J. Climatol.,* **30,** 1416–1422, doi:10.1002/joc.1961.

Sarma, V. V. S. S., T. Saino, K. Sasaoka, Y. Nojiri, T. Ono, M. Ishii, H. Y. Inoue, and K. Matsumoto, 2006: Basin-scale pCO_2 distribution using satellite sea surface temperature, Chl *a*, and climatological salinity in the North Pacific in spring and summer. *Global Biogeochem. Cycles,* **20,** GB3005, doi:10.1029/2005GB002594.

Scambos, T., H. A. Fricker, C.-C. Liu, J. Bohlander, J. Fastook, A. Sargent, R. Massom, and A.-M. Wu, 2009: Ice shelf disintegration by plate bending and hydro-fracture: Satellite observations and model results of the 2008 Wilkins ice shelf break-ups. *Earth Planet. Sci. Lett.,* **280,** 51–60.

Schaaf, C. B., and Coauthors, 2002: First operational BRDF, albedo nadir reflectance products from MODIS. *Remote Sens. Environ.,* **83,** 135–148.

Schlax, M. G., D. B. Chelton, and M. H. Freilich, 2001: Sampling errors in wind fields constructed from single and tandem scatterometer datasets. *J. Atmos. Oceanic Technol.,* **18,** 1014–1036.

Schmetz, J., 1989: Towards a surface radiation climatology: Retrieval of downward irradiance from satellites. *Atmos. Res.,* **23,** 287–321.

——, 1991: Retrieval of surface radiation fluxes from satellite data. *Dyn. Atmos. Oceans,* **16,** 61–72.

——, 1993: On the relationship between solar net radiative fluxes at the top of the atmosphere and at the surface. *J. Atmos. Sci.,* **50,** 1122–1132.

Scott, J. P., 2011: An intercomparison of numerically modeled flux data and satellite-derived flux data for warm seclusions. M.S. thesis, Dept. of Earth, Ocean and Atmospheric Science, The Florida State University, 75 pp. [Available online at http://etd.lib.fsu.edu/theses/available/etd-05242011-121615/.]

Serreze, M. C., and C. M. Hurst, 2000: Representation of mean Arctic precipitation from NCEP–NCAR and ERA reanalyses. *J. Climate,* **13,** 182–201.

——, A. P. Barrett, and F. Lo, 2005: Northern high-latitude precipitation as depicted in atmospheric reanalyses and satellite retrievals. *Mon. Wea. Rev.,* **133,** 3407–3430.

Shawstack, R., 2012: Arctic sea ice minimum extent. *Eos, Trans. Amer. Geophys. Union,* **90,** 388.

Shi, Y., and C. N. Long, 2004: Techniques and methods used to determine the best estimate of total downwelling shortwave radiation. *Proc. 14th Atmospheric Radiation Measurement (ARM) Science Team Meeting,* Albuquerque, New Mexico, 9 pp. [Available online at www.arm.gov/publications/proceedings/conf14/extended_abs/shi-y.pdf.]

Smith, K. L., P. J. Kushner, and J. Cohen, 2011: The role of linear interference in northern annular mode variability associated with Eurasian snow cover extent. *J. Climate,* **24,** 6185–6502.

Smith, S. D., 1988: Coefficients for sea surface wind stress, heat flux, and wind profiles as a function of wind speed and temperature. *J. Geophys. Res.,* **93** (C12), 15 467–15 472.

——, and Coauthors, 1992: Sea surface wind stress and drag coefficients: The HEXOS results. *Bound.-Layer Meteor.,* **60,** 109–142.

Smith, S. R., P. J. Hughes, and M. A. Bourassa, 2010: A comparison of nine monthly air–sea flux products. *Int. J. Climatol.,* **31,** 1002–1027, doi:10.1002/joc.2225.

Stackhouse, P. W., Jr., S. K. Gupta, S. J. Cox, T. Zhang, J. C. Mikovitz, and L. M. Hinkelman, 2011: 24.5-year SRB data set released. *GEWEX News,* No. 1, International GEWEX Project Office, Silver Spring, MD, 10–12.

Strong, C., G. Magnusdottir, and H. Stern, 2009: Observed feedback between winter sea ice and the North Atlantic Oscillation. *J. Climate,* **22,** 6021–6032.

Strow, L. L., and S. E. Hannon, 2008: A 4-year zonal climatology of lower tropospheric CO_2 derived from ocean-only Atmospheric Infrared Sounder observations. *J. Geophys. Res.,* **113,** D18302, doi:10.1029/2007JD009713.

Sverdrup, H. U., 1937: On the evaporation from the ocean. *J. Mar. Res.,* **1,** 3–14.

Taylor, P. K., and M. J. Yelland, 2001: The dependence of sea surface roughness on the height and steepness of the waves. *J. Phys. Oceanogr.,* **31,** 572–590.

Trenberth, K. E., J. T. Fasullo, and J. Kiehl, 2009: Earth's global energy. *Bull. Amer. Meteor. Soc.,* **90,** 311–323.

Trull, T. W., E. Schulz, S. G. Bray, L. Pender, D. McLaughlan, B. Tilbrook, M. Rosenberg, and T. Lynch, 2010: The Australian Integrated Marine Observing System Southern Ocean Time Series facility. *Proc. OCEANS '10,* Sydney, NSW, Australia, IEEE, 1–7, doi:10.1109/OCEANSSYD.2010.5603514.

Turner, D. D., and E. J. Mlawer, 2010: Radiative Heating in Underexplored Bands Campaigns (RHUBC). *Bull. Amer. Meteor. Soc.,* **91,** 911–923.

Vancoppenolle, M., and Coauthors, 2011: Assessment of radiation forcing data sets for large-scale sea ice models in the Southern Ocean. *Deep-Sea Res. II,* **58,** 1237–1249, doi:10.1016/j.dsr2.2010.10.039.

Waliser, D., and M. Moncrieff, 2008: The YOTC Science Plan. World Meteorological Organization Rep. WMO/TD-1452, WCRP 130, WWRP/THORPEX-9, 26 pp.

Wang, H., and R. T. Pinker, 2009: Shortwave radiative fluxes from MODIS: Model development and implementation. *J. Geophys. Res.,* **114,** D20201, doi:10.1029/2008JD010442.

Wanninkhof, R., W. E. Asher, D. T. Ho, C. Sweeney, and W. R. McGillis, 2009: Advances in quantifying air-sea gas exchange and environmental forcing. *Annu. Rev. Mar. Sci.,* **1,** 213–244.

Weissman, D. E., and M. A. Bourassa, 2011: The influence of rainfall on scatterometer backscatter within tropical cyclone environments—Implications on parameterization of sea-surface stress. *IEEE Trans. Geosci. Remote Sens.,* **49,** 4805–4814, doi:10.1109/TGRS.2011.2170842.

Whitlock, C. H., and Coauthors, 1995: First global WCRP shortwave surface radiation budget dataset. *Bull. Amer. Meteor. Soc.,* **76,** 905–922.

Wielicki, B. A., R. D. Cess, M. D. King, D. A. Randall, and E. F. Harrison, 1995: Mission to planet Earth: Role of clouds and radiation in climate. *Bull. Amer. Meteor. Soc.,* **76,** 2125–2153.

——, B. R. Barkstrom, E. F. Harrison, R. B. Lee III, G. L. Smith, and J. E. Cooper, 1996: Clouds and the Earth's Radiant Energy System (CERES): An Earth Observing System experiment. *Bull. Amer. Meteor. Soc.,* **77,** 853–868.

Wilson, E. L., E. M. Georgieva, and W. S. Heaps, 2007: Development of a Fabry–Perot interferometer for ultra-precise measurements of column CO_2. *Meas. Sci. Technol.,* **18,** 1495, doi:10.1088/0957-0233/18/5/040.

Woolf, D. K., 2005: Parameterization of gas transfer velocities and sea-state-dependent wave breaking. *Tellus,* **57B,** 87–94.

Wunsch, C., R. M. Ponte, and P. Heimbach, 2007: Decadal trends in sea level patterns: 1993–2004. *J. Climate,* **20,** 5889–5911.

Xie, P., and P. A. Arkin, 1997: Global precipitation: A 17-year monthly analysis based on gauge observations, satellite estimates, and numerical model output. *Bull. Amer. Meteor. Soc.,* **78,** 2539–2558.

Yang, D., 1999: An improved precipitation climatology for the Arctic Ocean. *Geophys. Res. Lett.,* **26,** 1525–1528.

Yelland, M. J., B. I. Moat, P. K. Taylor, R. W. Pascal, J. Hutchings, and V. C. Cornell, 1998: Wind stress measurements from the open ocean corrected for airflow distortion by the ship. *J. Phys. Oceanogr.,* **28,** 1511–1526.

——, R. W. Pascal, P. K. Taylor, and B. I. Moat, 2009: AutoFlux: An autonomous system for the direct measurement of the air-sea fluxes of CO_2, heat and momentum. *J. Oper. Oceanogr.,* **2,** 15–23.

Yuan, X., and C. Li, 2008: Climate modes in southern high latitudes and their impacts on Antarctic sea ice. *J. Geophys. Res.,* **113,** C06S91, doi:10.1029/2006JC004067.

Zhang, Y., W. B. Rossow, A. A. Lacis, V. Oinas, and M. I. Mishchenko, 2004: Calculation of radiative fluxes from the surface to top of atmosphere based on ISCCP and other global data sets: Refinements of the radiative transfer model and the input data. *J. Geophys. Res.,* **109,** D19105, doi:10.1029/2003JD004457.

Zhao, W., W. R. Kuhn, and S. R. Drayson, 1994: The significance of detailed structure in the boundary layer to thermal radiation at the surface in climate models. *Geophys. Res. Lett.,* **21,** 1631–1634.